Study on calibration stability and image sequence consistency in experimental 2.5-minute MSG rapid scan experiments

Authors:
Ján Kaňák, Slovak Hydrometeorological Institute, Jeséniova 17, 83315 Bratislava, Slovakia
Johannes Müller, EUMETSAT
Date: 9 January 2014 – 4 March 2014

Background of rapid scan experiments by MSG satellites

The initial 2.5-minute super rapid scan with MSG-3 was performed on 11-12 September 2012 during the MSG-3 satellite commissioning. This experiment was carried out upon recommendation of the *Convection Working Group*, which is a joint initiative of EUMETSAT and the *European Severe Storms Laboratory (ESSL)*.
Based upon recommendations of the STG-SWG and STG-OPSWG, the Secretariat has approved additional similar experiments which were done with the Meteosat-8 (MSG-1) satellite, pending confirmation of the health and safety aspects of such custom rapid scanning on the Meteosat-8 SEVIRI scan mechanism. Dates of all experiments were proposed by ESSL and are listed in table 1.

Table 1: List of super-rapid scan experiments

N	Satellites in parallel Intervals between images Satellite's position	Start date and time End date and time	Number of slots measured by satellites in parallel for 2.5 5 15 minutes
1	MSG3 MSG1 MSG2 2.5 5 15 3.4W 9.5E 0E	2012/09/11 09:00- -2012/09/12 08:55	575 288 96
2	MSG1 MSG2 MSG3 2.5 5 15 3.5E 9.5E 0E	2013/05/17 09:07- -2013/05/17 21:00	282 141 47
3	MSG1 MSG2 MSG3 2.5 5 15 3.5E 9.5E 0E	2013/06/17 09:00- -2013/06/17 21:00	289 145 49
4	MSG1 MSG2 MSG3 2.5 5 15 3.5E 9.5E 0E	2013/06/20 09:00- -2013/06/20 21:00	289 145 49
5	MSG1 MSG2 MSG3 2.5 5 15 3.5E 9.5E 0E	2013/07/29 09:00- -2013/07/29 21:00	289 145 49

Description of the method for image sequence consistency checks

Time interval between two consecutive images of Meteosat satellites (MSG series) depends on service provided. For essential 0 degree longitude service time interval is 15 minutes. For operational rapid scan service at 9.5E longitude time interval is 5 minutes and for experimental super rapid scans time interval is 2.5 minutes. Position of satellite was 3.4W during first experiment and 3.5E during next four experiments. Resulting from satellite positions also angular distance varied from 3.4° to 12.9° which should be considered when images are remapped and compared with respect to solar illumination and Earth-atmosphere as anisotropic radiance system.

While space or pixel resolution is the same for all three types of services, there is quite different time resolution. When we consider speed of clouds movement or development, than for lower scanning time interval we observe smaller changes of cloud positions and shapes. These changes can be monitored comparing two consecutive pictures in terms of statistical comparison of image pixel values. The simplest statistical parameters calculated can be: mean value of image pixels, standard deviation, bias or correlation coefficient. These parameters can be calculated for certain image subarea defined by user. In this study we decided to use mean image values and correlation coefficient of brightness temperatures in case of IR 10.8μm and albedos in case of HRV channel. Standard validation software developed at SHMU for statistical calculations in the frame of H-SAF precipitation validation cluster was used to calculate above mentioned statistical parameters. Additional parameter which was investigated in this study is amplitude and direction of image drifts resulting from satellite shaking or wobbling. Such drifts can be detectable using calculations of clear air areas (=cloud free areas) mass centers.

Processing of MSG HRIT SEVIRI image for all MSG satellites (MSG-1, 2, 3) into binary files was done using SHMU in-house MSGProc software. Brightness temperatures BT in [K] for IR 108μm and albedo in [%] for HRV channel are the output data from this processing; stored in 16-bit representation as an image of size 2000x1500 pixels, in Albers equal area projection (see Figure 4, left). Parameters of projection were pre-set with the aim to avoid the losses of native resolution of SEVIRI pixels. Some distortions of scan lines could affect the results which were taken into account in conclusions.

Mean BT calculations over the image area (bordered by limits x>=240, x<=1700, y>=140, y<=1200 from total 2000x1500 image size) for each timeslot and each satellite were proceed and BT differences for each satellite pair (2.5-5, 2.5-15, 5-15 minutes scans) were derived. To complete satellites data pairs for each 2.5-minute timeslot with longer scan periods (5-min and 15 minutes) values were not interpolated but simply repeated for nearest 2.5-minute interval.

Correlation between two consecutive images was calculated for couples of images in following time order:

2.5-minutes scan: couples 9:00-9:02, 9:02-9:05, 9:05-9:07, ... up to end of experiment

5-minutes scan: couples 9:00-9:05, 9:05-9:10, 9:10-9:15, ... up to end of experiment

15-minutes scan: couples 9:00-9:15, 9:15-9:30, 9:30-9:45, ... up to end of experiment

Similarly to mean image values correlation values for 2.5-minutes slots in between 5 and 15 minutes intervals were repeated without interpolation.

Repetition of values for 2.5-minute timeslots in-between 5 and 15-minutes scans is the reason of jumps – sawing character (zigzag) of plotted lines (e.g. lines in Figures 2.4, 2.5, 2.6,…), but in general applicable enough to compare data from various satellites and interpret the results correctly.

Image drifts or shaking was detected using floating window extracted from the first image from time slot T_0 which floats over the second image from next time slot T_1=T_0+2.5[5, 15]minutes, calculation of correlation for different positions of floating window and selection of the position with maximum of correlation. Coordinates of the center of floating window in the second image with maximum correlation correspond to the mutual images drift. Equivalent for such calculations is image convolution filter.
Because of data amount and limited calculation resources evaluation of image drifts was done also by calculation of mass center coordinates of the image or its part. In our case calculations must be done for cloud-free areas (land surface patterns) of image to avoid disturbing movement and changes of clouds in time. For this purpose we prepared cloud-free area masks for each RSS experiment.

Preparation of clear area mask:

- Average, minimum and maximum HRV and IR imagery was calculated for selected timeslots
- More RGB combinations (HRV max, HRV avg, IR min, HRV max, HRV max, IR max,…) were tested
- HRV max, HRV avg and IR max combination was selected for visual identification of cloud-free areas
- Visual identification was done manually in Photoshop-like editor

Example of clear area mask is shown in Figure 1.

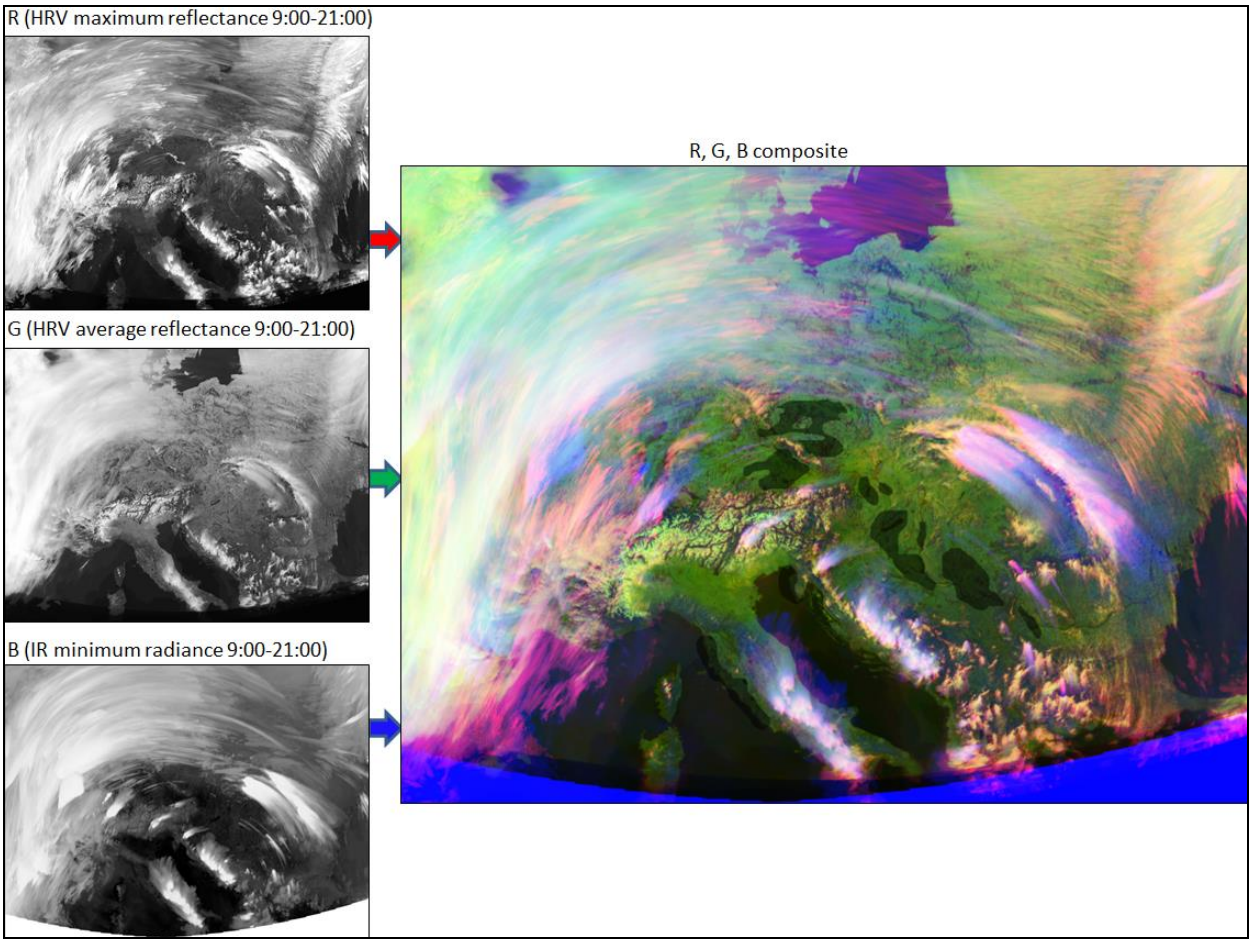

Figure 1: 17 June 2013, 9:00 – 21:00 UTC composite image and visual detection of cloud-free areas for image drift calculations during the selected period.

Image drift calculations: For an object in a gray scale image, its *center of mass* is the point around which the gray of the object is equally distributed. In our case mass center coordinates were calculated for each image timeslot according cloud-free area masks using formula:

$$\mathbf{R} = \frac{1}{M}\sum_{i=1}^{n} m_i \mathbf{r}_i$$

HRV pixel albedo and/or IR BT values were used instead of m_i weights, vector r_i was separated into x_i and y_i components. Mass center coordinates were calculated separately for x_i and y_i in EW and NS directions and for each timeslot (i=9:00 to 21:00UTC with step 2.5 [5, 15] minutes).

Then relative image shift between consecutive time slots was calculated as:

$$\Delta x_i = x_i - x_{i-1} \quad \Delta y_i = x_i - x_{i-1} \quad \text{and} \quad \Delta R_i = \mathrm{sqrt}(\Delta x_i^2 + \Delta y_i^2)$$

Finally, extremes in consecutive image shifts were estimated calculating changes of the second order:

$$\Delta^2 R_i = \Delta R_i - \Delta R_{i-1}$$

Results of calculations are shown in image drift plots in Annex 1 (e.g. Figures 1.8, 2.8, …).

To compare time changes in image sequence between different satellites we performed the same calculation for parallel services as it is listed in the first column of Table 1. Statistical parameters were calculated for the entire period of experiment and for 3 different areas (see Figure 2) defined as follows:

- Full image area with emphasis on central European region (red box)
- Subarea of clouds individually positioned according meteorological situation (blue box)
- Subarea of cloud-free regions individually selected according meteorological situation (green box)

Because the calibration of SEVIRI instrument could not be performed during RSS experiments, subareas were selected with the aim to test how precise was calibration of MSG channels during RSS experiment for low, high and overall radiances and how they varied in time in comparison to other MSG services.

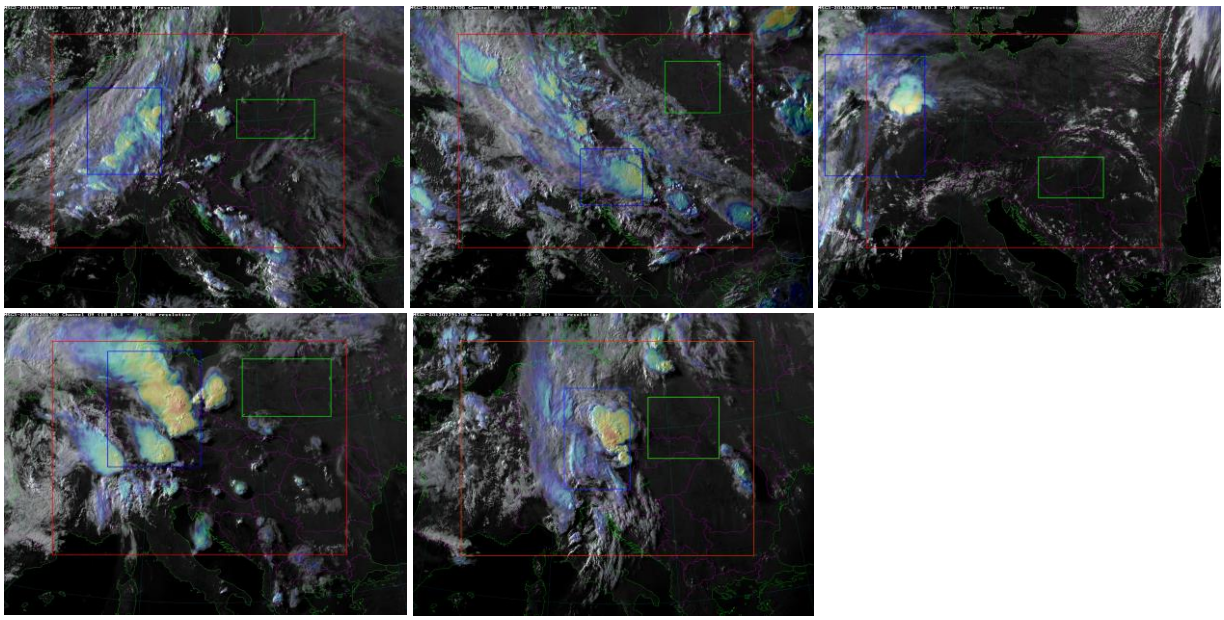

Figure 2: HRV sandwich products with image areas predefined for statistical calculations – red box for full image area, blue box for clouds and green for clear atmosphere. From left to the right: 11 September 2012 15:30, 17 May 2013 17:00, 17 June 2013 11:00 in upper line, 20 June 2013 17:00 and 29 July 2013 17:00 UTC in bottom line.

Results of data analyses

We processed all available time slots from all 3 MSG satellites for all 5 super RSS experiments. Output data from processing were used to plot set of charts which are attached to this document as ANNEX 1. Here we will summarize the results for each RSS experiment and discuss in details some special effects which were identified.

General description of the charts

Correlation coefficients show time consistency of IR 10.8µm and HRV image time sequences. Values displayed in charts correspond to the full image area, blue line to 2.5-minute scan, red line to 5-minute scan and green line to 15-minute scan. **Correlation values for 2.5-minute scans are the highest and for 15 -minutes scans are the lowest, which result from time image changes.** While changes in the image (movement and development of cloud fields) for 15-minute intervals are high and correlation is lower, changes for 2.5-minute scan intervals are lower and correlation is higher. Therefore dependence of correlation on weather situation in 2.5-minute scans is very low, but in 15-minute scans we can observe high correlation variability resulted from changes of cloud fields. In case of 2.5-minute scan we can observe often the technical performance of the satellite and scanning instrument. Performance of image navigation and rectification can be observed as certain small discontinuities of correlation in time. Sensitivity of the method is high enough to reflect discontinuities of small significance and reflect standard variations of image reprocessing from level 1 to 1.5. Therefore it is important to recognize and differentiate between standard and extra ordinal discontinuities. To highlight the correlation variability for 2.5-minute scans these values were plotted into charts in narrow scale interval according the right side scale of the charts (0.9 to 1.0 for HRV and 0.985 to 1.0 for IR channel). In opposite correlation values for 5 and 15-minutes scans were plotted in wider scale interval according left side scale of the chart (0.7 to 1.0 for HRV and 0.9 to 1.0 for IR channel).
Time changes in correlation are useful to demonstrate how scanning instrument, satellite and image navigation were stable during the experiment. In general our study showed that performance was of high stability, only in some cases we observed regular periodic changes in correlation with the period of 30 minutes or even non-periodical chaotic disturbances which evidently did not correspond to any meteorological change of image scene.

Mean image values of IR 10.8µm and HRV channels show differences in calibration between all three satellites measured the same scene at the same time in parallel. Mean values were calculated separately for 3 different areas and were plotted by green (clear atmosphere), blue (cloudy) and red (full image) color lines in the charts. Different line style was used for each scan time interval (dotted for 2.5, dashed for 5 and solid line for 15 minute time interval). It is important to note that HRV values are not representative close to the terminator and mean values are going down during sunset or are growing up during sunrise. Again we stress the fact that during experiments onboard calibration of SEVIRI instrument could not be performed, therefore knowledge/assurance of calibration stability is important.

Mean differences of IR 10.8μm and HRV channel values are displayed in charts for three different areas – red line for full image area, blue line for cloudy and green line for cloud-free areas. To minimize number of plots only differences between 2.5 and 5 minutes scans were put into charts. Differences for IR channel varies in interval -1/+1 K, differences for HRV albedo varies from -10% to 8%. The most useful information available from mean differences is their time development during the experiment. The Earth/atmosphere system is mostly non-isotropic. This fact is true especially for visible but also for infrared radiation. When talking about different viewing angles of satellite instrument, it means there is also different path of the radiation through the atmosphere.

The uncertainty of the SEVIRI calibration is expected in the order of 1 K, the maximum allowed drift between two calibrations is 0.05K. As there are no calibrations for 2.5 min scans (but there are hourly calibrations for 5 and 15 minute scans), one would need to analyse the drift for 24 hours for Meteosat 8 in that period. Currently, we found only a drift of 0.04% of the gain per day.

Daily variations which can be found in Figures 1.5, 1.6, 2.5, 2.6, 3.5, 3.6, 4.5, 4.6, 5.5 and 5.6 of Annex 1 can be completely explained by anisotropy character of measured scenes, Sun elevation and mutual angular distance between satellite and Sun. **When we compare differences between all MSG satellites, stability of mean IR BT and VIS albedo over the scene is very high**.

Image drift plots for HRV imagery show movement of cloud-free area mass centers changes of their coordinates in horizontal (EW) and vertical (NS) directions (figures x.7 of Annex 1). If there is not observed any image drift, lines for EW and NS directions are smooth and values are around zero. In case of detectable image drift we observe short disturbances in one or both directions. To detect extreme image disturbances we used principle of 2nd order of difference. It means that we calculated differences of cloud-free mass center's position changes between two successive timeslots (figures x.8 of Annex 1).

Detailed results case by case

Case 11-12 September 2012 (24 hours experiment)

Super rapid scan was done by satellite MSG-3 during its commissioning phase. 5-minutes RSS was done by MSG-1 and 15-minutes scan by MSG-2 satellites in this case. Consistency checks showed clearly high quality of 2.5-minute MSG-3 data and high performance during measurements (in comparison to next super RSS experiments in 2013 done by MSG-1 satellite).

Correlation between two consecutive images (charts 1.1 and 1.2 in Annex 1) shows stable and contiguous changes of image scenes in time. Only few timeslots of 2.5 minutes scans in comparison to 5 minutes scans show smaller balance, namely timeslots:

- 11/09/2012 11:30 UTC
- 11/09/2012 23:45 UTC
- 12/09/2012 00:25-00:47 UTC
- 12/09/2012 06:50-07:27 UTC

Mean values (charts 1.3 and 1.4 in Annex 1) show slight differences in calibration between all three satellites. Mainly from the beginning of experiment 2.5-minute IR BT were 2K lower than 5-minute IR BT. From 11.9.2012 19:50 UTC to 12.9.2012 02:00 UTC mean difference was around zero and then difference

reached again -2K at the end of experiment. In case of clear area IR BT difference reached -3K as it is shown in chart 1.5 in Annex 1). We noted also that difference of warm clear areas between 12:00-15:00UTC were lower than differences for cold cloudy areas. In other words dynamic range of IR 10.8µm sensor slightly changed during the whole experiment but also anisotropy effects were intensified due to big orbital difference of satellites in this case (3.4W and 9.5E = 12.9°).
Differences of albedo for HRV channel (chart 1.6 in Annex 1) for 2.5-minute scan in comparison to 5-minute scan were 6% lower from the beginning, than reached zero at 14:00 UTC and before sunset reached +2%. Next day morning differences were again negative and at the end of experiment reached -6%.
Image drifts (charts 1.7 and 1.8) derived from movement of cloud-free area mass centers did not exceed level of 0.2 pixels per timeslot therefore **we consider this RSS case as free of image drifts and of high quality of image rectification** for all time slots.

Case 17 May 2013 (12 hours experiment)

This 2.5-minute scan experiment (and next 3 experiments in 2013) was done by satellite MSG-1, 5-minutes RSS by MSG-2 and MSG-3 provided essential 15-minutes service.
Correlation changes in time are shown in chart 2.1 (IR) and 2.2 (HRV). There is evident high time variability of image data. When we compare all three satellites, we can differentiate between long time changes due to weather situation and short time changes probably caused by satellite and scan mechanism stability. Short time changes are periodical and certain maxima and minima of image correlation can be identified:
Minima at 9:35, 10:07, 10:35, 11:07, 11:37, … 16:05, 16:37, 17:07,17:37, 18:05, 18:37,…
Maxima at 9:47, 10:15, 10:55, 11:30, … 17:00, 17:27, 17:57, 18:25, 18:50, 19:22,…
Relative position of minimums and maximums is asymmetric, but we can observe regular time intervals between minimums 30 minutes and the same intervals between maximums. Possible explanation of this periodicity can be wobbling of satellite platform, but it is unclear why the period is 30 minutes, while SEVIRI instrument was constructing primarily for 15-minute full Earth disk scan.
It is important to note, that no similar periodicity was found in case of MSG-3 satellite during first super RSS experiment.
Variability of correlation can be observed also in HRV channel, but noisier due to different image resolution, cloud shadows in the image, sun elevation and other effects.
Calibration of IR 10.8µm and HRV channels during experiment was stable, as can be seen in charts 2.3 and 2.4 of Annex 1.
Mean IR differences (chart 2.5) varied from -0.5K to +0.5K during whole 12-hour period of experiment. Mean albedo differences (chart 2.6) varied from -2% to +2%. Anisotropy effects between 2.5 and 5-minutes data are not so significant in this case because of lower satellites orbit distance 6° (3.4W and 9.5E).
Image drifts (charts 2.7 and 2.8) derived from movement of cloud-free area mass centers reached level of 0.2 pixels per timeslot and for time slot 14:15UTC exceed this level to value 0.4, which is not

significant. Therefore **we consider also this RSS case as stable and of good quality of image rectification** for all time slots.

Case 17 June 2013 (12 hours experiment)

This 2.5-minute scan experiment was done by satellite MSG-1, 5-minutes RSS by MSG-2 and MSG-3 provided essential 15-minutes service.

Correlation changes in time are shown in chart 3.1 (IR) and 3.2 (HRV). There is also evident high time variability of image data, but periodical changes can be recognized only with difficulties. We found few extremely low values of correlation for following dates: 10:10, 13:02, 14:30, 16:17 and 19:00 UTC, for both IR and HRV channels. Therefore we suppose that wobbling of satellite in this experiment was irregular and with higher maximum amplitude.

Calibration of IR 10.8μm and HRV channels during this experiment was stable, as can be seen in charts 3.3 and 3.4 of Annex 1.

Mean IR differences (chart 3.5) varied from -0.4K to +0.5K during whole 12-hour period of experiment. Higher differences than +1K were observed only for cloudy areas from 15:00 to 18:30 UTC. Mean albedo differences (chart 3.6) varied in narrow interval from -1% to +1%. We can note very stable performance of HRV channel in this case.

Image drifts (charts 3.7 and 3.8) derived from movement of cloud-free area mass centers we detected higher, between 0.2 to 0.6 pixels per timeslot. Over more for some time slots we detected drifts which can have impact for precise localization of small-scale meteorological objects, namely:

Time slot UTC	Size of drift in pixels:
12:47	1.8
13:05	1.0
14:27	1.2
14:32	1.6
15:07	0.7
17:02	2.2

By visual inspection of the images from selected timeslots (see Figure 3) we found strong east-west image shifts in the south part of the image. Shifts can be observed over south Italy, Sardinia and Albania. In spite of the fact that our cloud-free area mask (Figure 1) is situated more to the north, algorithm for image math center is sensitive to such disturbances and confirms that image quality is lover not only in the south part where it is detectable visually but over wider area of image.

In comparison to previous (and in general to all other) experiments **we consider this case as the case with the most disturbed image stability**. For precise localization of small-scale meteorological objects users should be careful especially for above listed time slots.

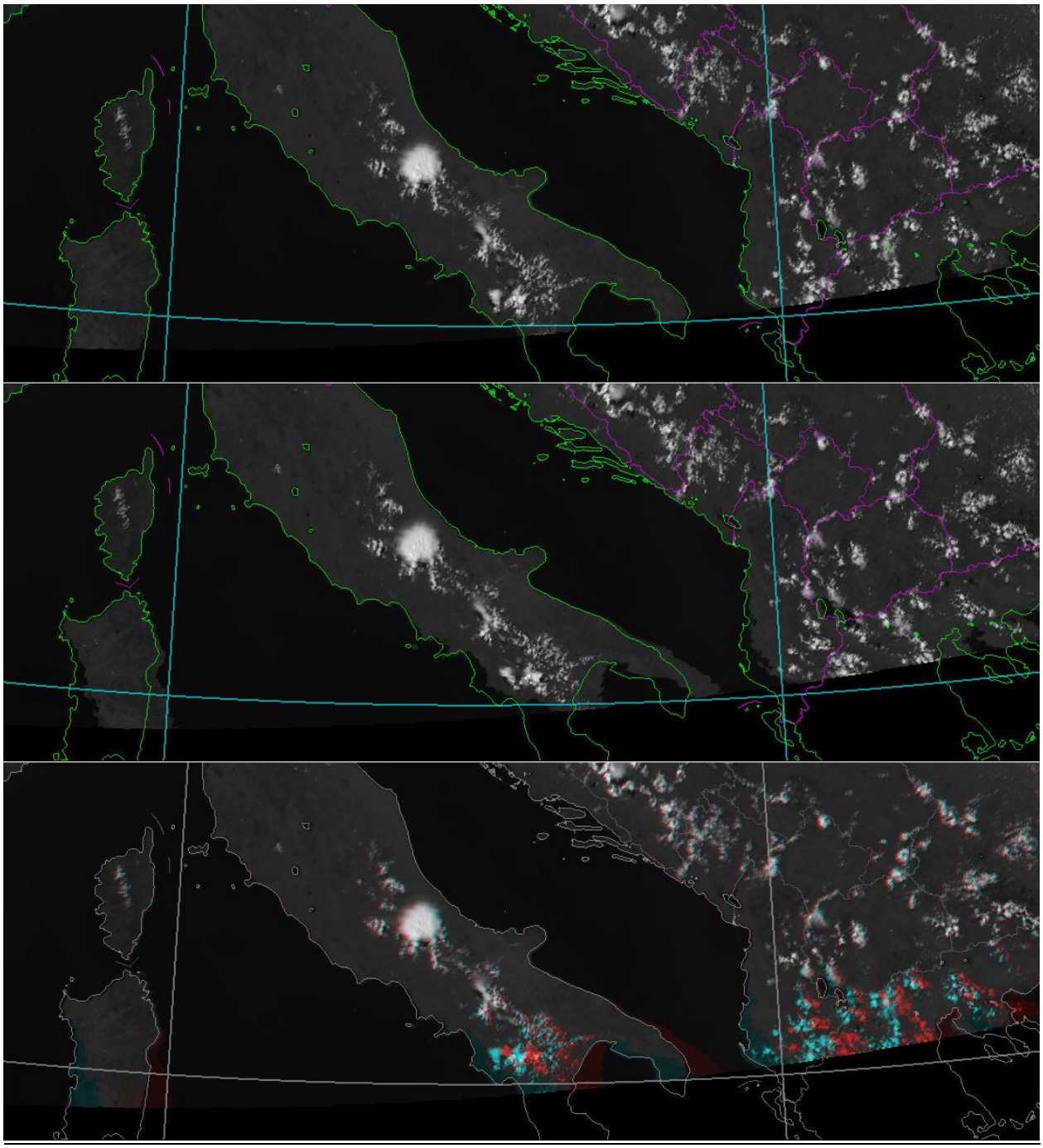

Figure 3: Example of East-West image drift in south part of image. Image on top is from 17 June 2013 12:45 UTC, in middle from 12:47 UTC and bottom image shows RGB composite of both images highlighting the amplitude of image line drifts in EW directions.

Case 20 June 2013 (12 hours experiment)

This 2.5-minute scan experiment was done by satellite MSG-1, 5-minutes RSS by MSG-2 and MSG-3 provided essential 15-minutes service.

In correlation time changes (charts 4.1 and 4.2 of Annex 1) we detected significant periodical minima and maxima for number of timeslots:
Minima at: 9:12, 9:35, 10:07, 10:37, 11:07, 11:37, 12:07, 12:37, 13:07, 13:35 UTC
Maxima at: 9:22, 9:47,, 10:25, 10:50, 11:22, 11:55, 12:15, 12:57, 13:20, 13:55 UTC
After 14:00 UTC amplitude between maxima and minima of correlation became lower but spacing of changes 30 minutes remained during the whole experiment. Explanation can be the same as it was in case of experiment from 17 May 2013 - wobbling of satellite body or scanning instrument.
Calibration of IR 10.8µm and HRV channels during this experiment was also very stable as can be seen in charts 4.3 and 4.4 of Annex 1.
Mean IR differences (chart 4.5) varied from -0.5K to +0.6K during whole 12-hour period of experiment. Differences were negative from 9:00 to 11:10 UTC, for the rest of experiment differences were positive. Mean albedo differences (chart 4.6) varied in narrow interval from -1% to +1.5%.
Image drifts (charts 4.7 and 4.8) derived from movement of cloud-free area mass centers reached in average level of 0.1 pixels per timeslot and only for time slot at 17:05UTC reached the value 0.2, which is not significant. Therefore **we consider this RSS case as stable and of very good quality of image rectification** for all time slots.

Case 29 July 2013 (12 hours experiment)

This 2.5-minute scan experiment was done by satellite MSG-1, 5-minutes RSS by MSG-2 and MSG-3 provided essential 15-minutes service.
Correlation changes in time are shown in chart 5.1 (IR) and 5.2 (HRV). Similarly to case 17 June 2013 there is also evident high variability of correlation in time and periodical changes can be recognized only with difficulties. Irregular disturbances of higher amplitude were observed for timeslots 15:05, 15:25, 18:00 and 20:17 UTC. Periodical changes with period of 30 minutes can be recognized only for few time slots: 10:37, 11:05, 11:37, 12:07, 12:35 and 13:07 UTC.
Calibration of IR 10.8µm and HRV channels during this experiment was also very stable as can be seen in charts 5.3 and 5.4 of Annex 1.
Mean IR differences (chart 5.5) were positive and varied from 0K to +0.6K. Only after 19:30 UTC mean difference became negative and reached values of -0.2K. Mean albedo differences (chart 5.6) varied in slightly wider interval from -2% to +2%. We observed also jumps of albedo at 9:55 and 13:43, but only for cloudy areas, caused probably by special Sun-clouds-satellite angle and related anisotropic effects.
Image drifts (charts 5.7 and 5.8) derived from movement of cloud-free area mass centers did not exceed level of 0.1 pixels per timeslot therefore **we consider this RSS case as very stable and of high quality of image rectification** for all time slots.

Note: Timeslots close to sunset were not considered for evaluation of image drifts on the base of HRV imagery. IR imagery also exhibits some increasing of drift parameters which relate mainly to gradual land surface temperatures in areas classified as cloud free.

Notes to observation of image drifts during 17 June 2013 measurements

The experiment 17 June 2013 was only the case when next-to sub-pixel drifts we detected short-time image drifts with amplitude of few pixels. Plot in Figure 4 (in the right) shows similarities in image mass center paths during the day for all MSG satellites and how image drifts differ from satellite to satellite. While for 15-minutes scan the path is very smooth, in 5-minutes scan we found few drifts of magnitude in average higher than 1 pixel and in 2.5-minutes scan we found more significant image drifts with averaged amplitude of 2 pixels per timeslot.

Area of plot in Figure 4 represents very small white box in the middle of processed domain (map in the left of Figure 3). Red arrows in the plot represent image drifts oriented in South-West direction. Image mass centers drift in fact over very small area of image (10x10 pixels) during the experiment.

When we divided cloud-free area mask into few subareas (Figures 5a, b, c, d and e) and calculated mass centers separately for individual subareas, we found out that some areas were drifted with higher and another with lower amplitudes. The most affected subarea was western part of Italy. Detailed analyses of cloud-free subareas and visual inspection of imagery showed that extreme shifts were detected in the same timeslots when extreme East-West shifts were observed in southern part of the image. In spite of the fact that cloud-free areas were selected to the north from affected parts of the image, we were able to detect 1 or 2 pixel image drifts in average over central parts of image. Over more such drifts are not visible by simple visual evaluation of image but can be detected only using numerical calculations.

We assume that drifts detected on processed level 1.5 image data can differ from raw level 1.0 image drifts, because image rectification done in real time is very complex process. For better understanding we provide here brief description of this process:

The processor needs to process in real time. That means it has to predict the conditions for image taking. This prediction contains mostly the information about orbit and attitude of the spacecraft, alignment of the SEVIRI instrument with the actual spin axis. Further input to the processor is what the spacecraft will be commanded in terms of the scan pattern (start of scan, duration of scan, retrace). From here it predicts where every pixel in the raw image will be in a perfectly centered image line.

During the scan, the image is resampling and disseminated. After the scan, landmarks are used to assess the quality of the prediction – or the model is used for the prediction based on the above mentioned factors. This landmark measurement is used to improve the model for the next scan.

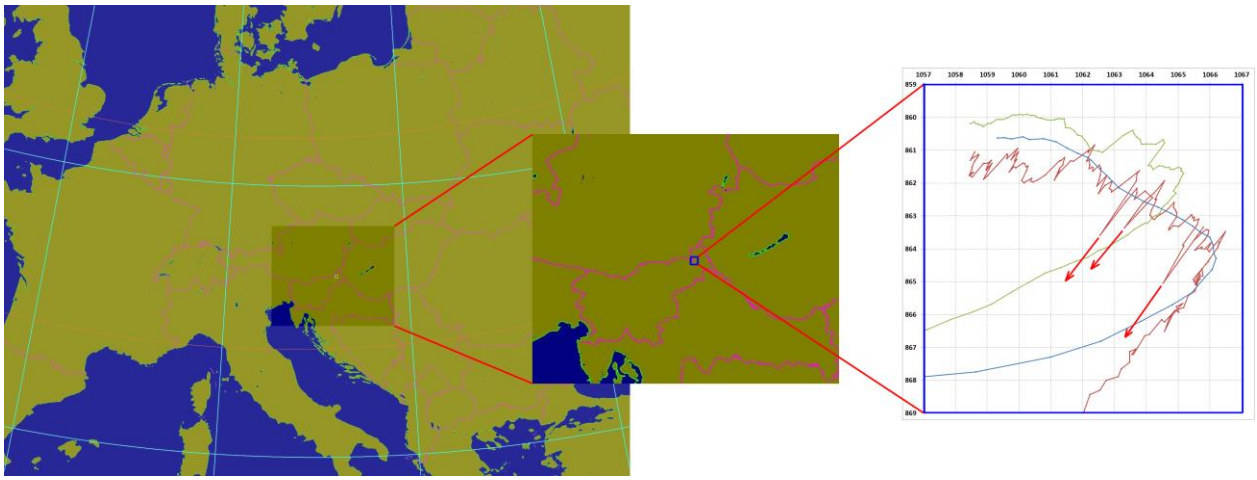

Figure 4: Path of clear air area mass center over image during 17 June 2013 experiment. Red line belongs to MSG-1 2.5-minutes data, green to MSG-2 5-minutes data and blue to MSG-3 15-minutes data.

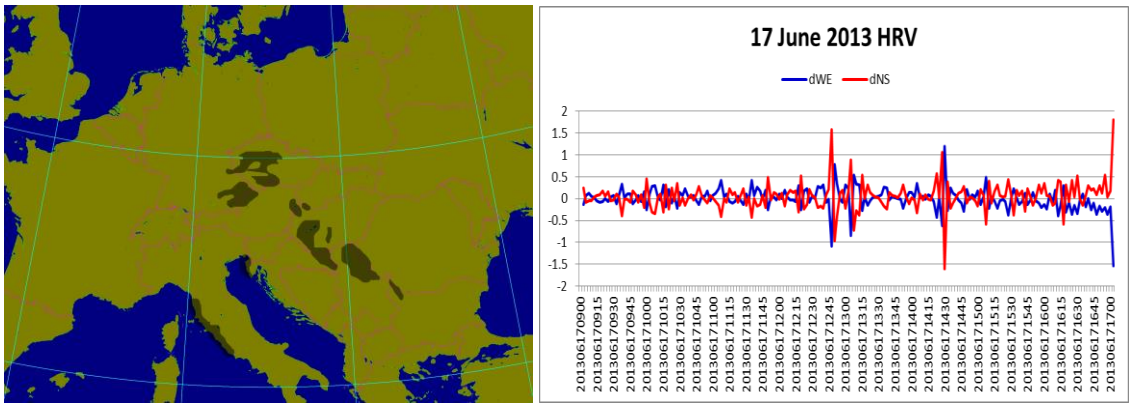

Figure 5a: Image drifts detected by mask for all selected cloud-free regions.

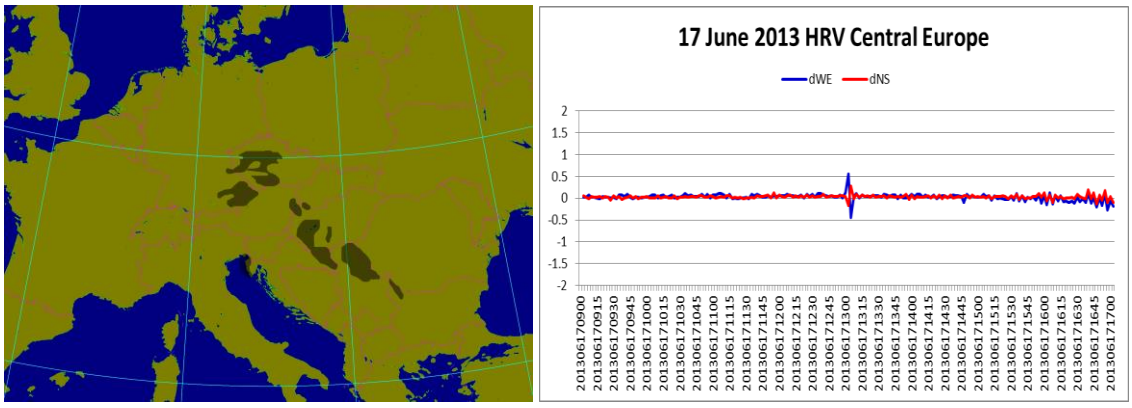

Figure 5b: Image drifts detected by mask for all selected cloud-free regions except west coast of Italy.

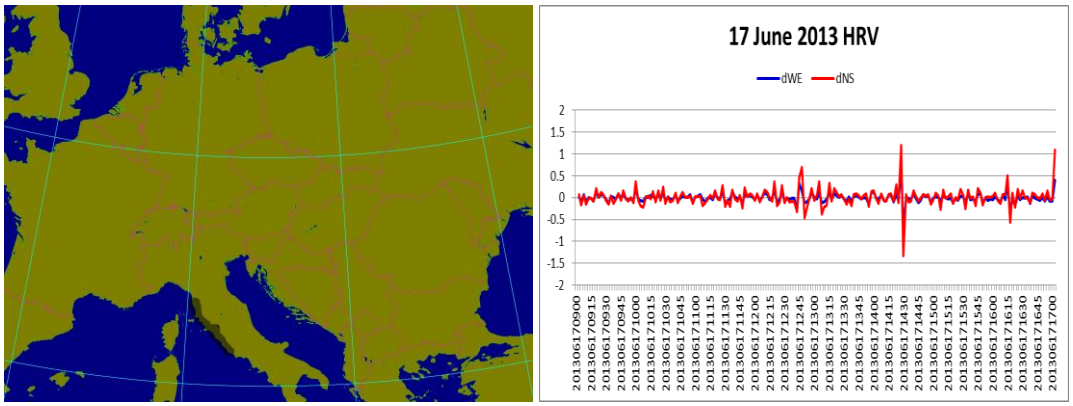

Figure 5c: Image drifts detected by mask for cloud-free regions of west coast of Italy.

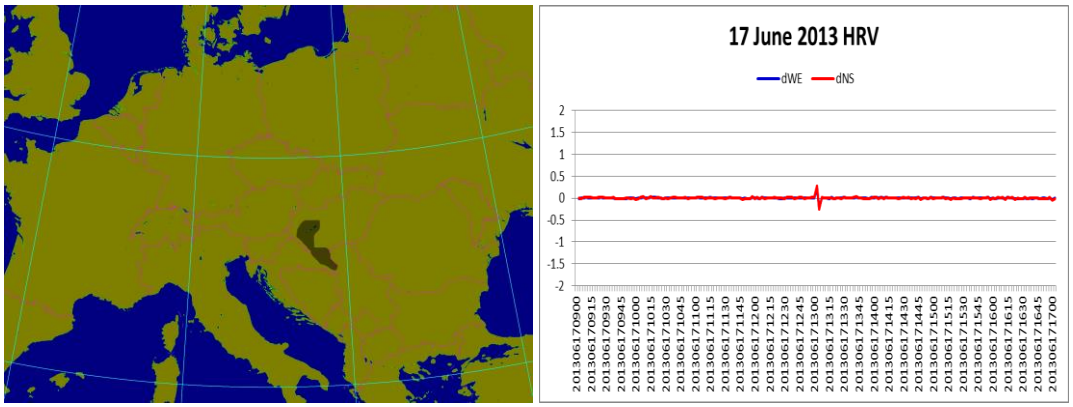

Figure 5d: Image drifts detected by mask for cloud-free regions of Hungary and East Croatia.

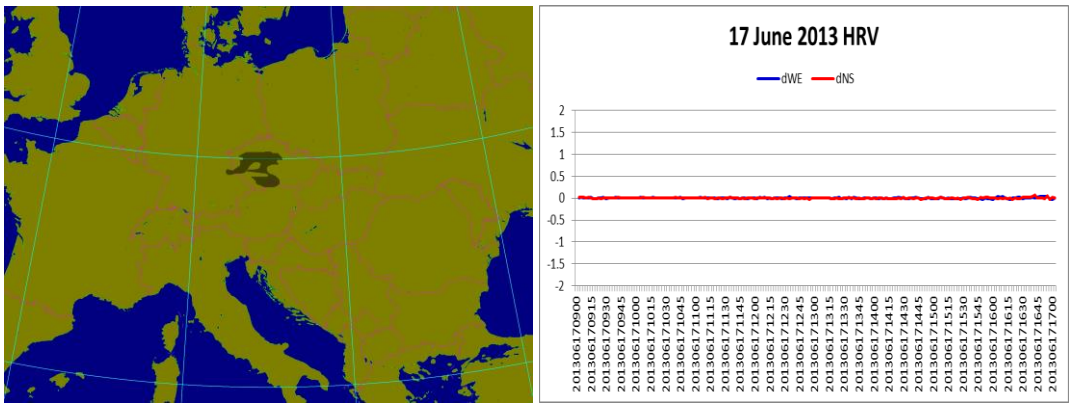

Figure 5e: Image drifts detected by mask for cloud-free regions of Czech Republic.

Comparison of cloud-free areas mass center drifts for all 2013 experiments is provided in Figure 6. We already noted that seasonal and daily changes of Sun illumination and anisotropy effects influence the behavior of cloud-free area mass centers calculation. Therefore shapes of daily path differ for different experiments, but shapes of path for satellite triplets for particular experiment are similar.

All plots represent the area of the same size 10x10 pixels. All trajectories start at 9:00 UTC close to the chart center, move with respect to the Sun illumination during the day and then during sunset escape from displayed area of plots.

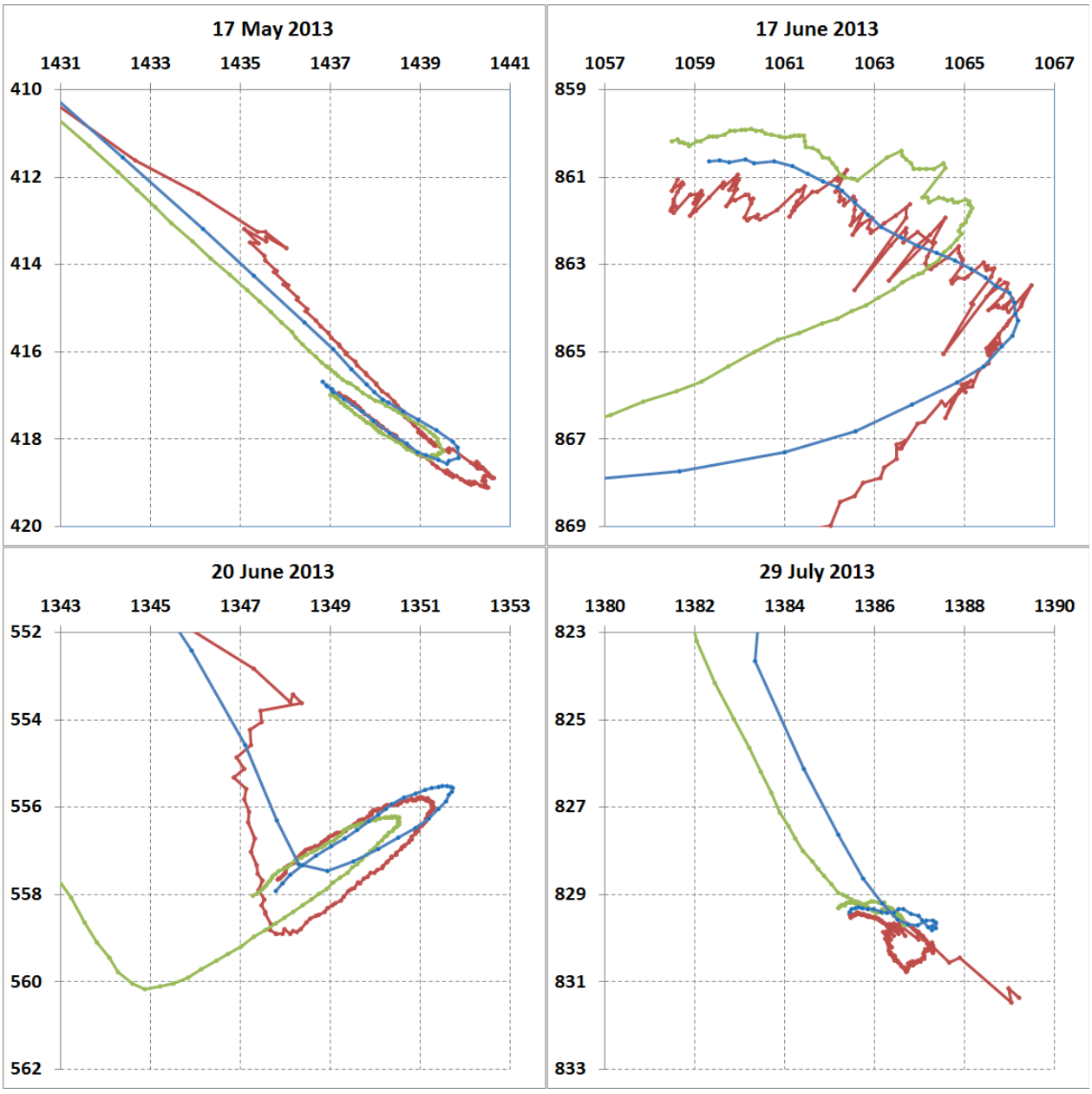

Figure 6: Comparison of the paths of clear air area mass centers over images during all 2013 RSS experiments. Red line belongs to MSG-1 2.5-minutes data, green to MSG-2 5-minutes data and blue to MSG-3 15-minutes data.

Conclusions

The analysis of the consistency between 15, 5 and 2.5 minute scans very much suffers from natural effects like anisotropy of the atmosphere. These effects exhibit mainly in the visible, but particularly also in the infrared part of the spectrum and were manifested regularly on daily base as changes in average values of radiance, brightness temperature and albedo. Course of these changes was slightly different for different experiments and corresponded to different inclination of the Earth's axis from season to season. Significant effects were observed even during the Sun set or Sun rise close to the terminator (twilight, changes of cloud-free area surface temperature). To avoid the big influence of about mentioned effects we validated BT differences between MSG satellites instead of average values. Daily variance of BT differences were in good agreement with nominal precision of sensor's calibration.

Calculation of the correlation between two successive frames showed regular periodic oscillations of the correlation values with a period of 30 minutes in case of 20 June 2013. In other cases from 2013 these periodic oscillations were recognised only with effort because they were often disturbed by irregular drifts of higher order. Similar oscillations were not observed during first experiment from 11 September 2012, which was done by MSG-3 satellite. We suppose that these periodical oscillations relate to technical status of MSG-1 satellite after 11 years of operations. The reason of discontinuities is wobbling of image in EW direction, namely the minimum of correlation is related to the fast jump of image in direction from West to East.

Explanation of irregular drifts was possible by detailed analyses of cloud-free area mass centres movement. By visual inspection of imagery we found out that extreme shifts of cloud-free area mass centres were detected in the same timeslots when extreme line shifts were observed in southern part of the image. In spite of the fact that cloud-free areas were selected northerly to avoid these parts of image (affected by return point of scan mechanism), we were able to detect 1 or 2 pixel drifts in average over central parts of images.

Detailed monitoring of mass center movement of cloud-free areas of the image showed that the experiments from 11 September 2012, 17 May 2013, 17 June 2013 and 29 July 2013 **provided very stable imagery with an average positional accuracy of 0.1 to 0.2 pixels**. **Only in the experiment from 17 June 2013 we have identified several more pronounced short-term image displacements with mean amplitude of 2 pixels per timeslot**.

In conclusion, the experimentally obtained 2.5-minutes super RSS data by MSG satellites are of high quality in terms of the calibration stability and geo-referencing, apart from a few timeslots of 17 June 2013, notably slots 10:10, 11:07, 11:40, 12:47, 13:05, 14:30, 16:07, 16:57 and 19:00. Also the slot 14:15UTC from 17 May 2013 shows noticeable image shift of value 0.4 pixel per slot. Image quality is significantly degraded sometimes in the south part of scanned area which is affected by return point of scan mechanism. Sensitive tests based on mass center movement of cloud-free areas showed that this EW image drifts are propagated over the all parts of image but with decreasing amplitude non-perceptible by visual observation.

From meteorological point of view small scale features of severe storms, namely overshooting tops observed in standard scan mode of MSG 15-minute imagery, exhibit random behaviour with observing time below scan time interval. But also in shorter scan intervals (5-minutes RSS and 2.5-minutes super RSS) this random behaviour retains observable. This was the reason why study of image calibration

stability, precision of navigation and rectification was considered important. **Identification of high image quality apart from several short-term image displacements identified for 17 June 2013 can be useful for confident usage of experimental data in any other studies**. Next shortening of scan time intervals should refer in future also to higher space resolution, which is promising by next generation of geostationary satellites in the frame of MTG program.

ANNEX 1

List of plots

1. Case 11-12 September 2012
   1.1. Correlation between two IR consecutive images for 15, 5 and 2.5min scans
   1.2. Correlation between two HRV consecutive images for 15, 5 and 2.5min scans
   1.3. Mean IR values for full image, cloudy and clear atmosphere areas for 15, 5 and 2.5min scans
   1.4. Mean HRV values for full image, cloudy and clear atmosphere areas for 15, 5 and 2.5min scans
   1.5. Mean IR 2.5-5min scans differences for full image, cloudy and clear atmosphere areas
   1.6. Mean HRV 2.5-5min scans differences for full image, cloudy and clear atmosphere areas
   1.7. Time changes of cloud-free area mass center coordinates derived from consecutive timeslots
   1.8. Detection of extreme shifts of cloud-free area mass centers
2. Case 17 May 2013
   2.1. Correlation between two IR consecutive images for 15, 5 and 2.5min scans
   2.2. Correlation between two HRV consecutive images for 15, 5 and 2.5min scans
   2.3. Mean IR values for full image, cloudy and clear atmosphere areas for 15, 5 and 2.5min scans
   2.4. Mean HRV values for full image, cloudy and clear atmosphere areas for 15, 5 and 2.5min scans
   2.5. Mean IR 2.5-5min scans differences for full image, cloudy and clear atmosphere areas
   2.6. Mean HRV 2.5-5min scans differences for full image, cloudy and clear atmosphere areas
   2.7. Time changes of cloud-free area mass center coordinates derived from consecutive timeslots
   2.8. Detection of extreme shifts of cloud-free area mass centers
3. Case 17 June 2013
   3.1. Correlation between two IR consecutive images for 15, 5 and 2.5min scans
   3.2. Correlation between two HRV consecutive images for 15, 5 and 2.5min scans
   3.3. Mean IR values for full image, cloudy and clear atmosphere areas for 15, 5 and 2.5min scans
   3.4. Mean HRV values for full image, cloudy and clear atmosphere areas for 15, 5 and 2.5min scans
   3.5. Mean IR 2.5-5min scans differences for full image, cloudy and clear atmosphere areas
   3.6. Mean HRV 2.5-5min scans differences for full image, cloudy and clear atmosphere areas
   3.7. Time changes of cloud-free area mass center coordinates derived from consecutive timeslots
   3.8. Detection of extreme shifts of cloud-free area mass centers
4. Case 20 June 2013
   4.1. Correlation between two IR consecutive images for 15, 5 and 2.5min scans
   4.2. Correlation between two HRV consecutive images for 15, 5 and 2.5min scans
   4.3. Mean IR values for full image, cloudy and clear atmosphere areas for 15, 5 and 2.5min scans
   4.4. Mean HRV values for full image, cloudy and clear atmosphere areas for 15, 5 and 2.5min scans
   4.5. Mean IR 2.5-5min scans differences for full image, cloudy and clear atmosphere areas
   4.6. Mean HRV 2.5-5min scans differences for full image, cloudy and clear atmosphere areas
   4.7. Time changes of cloud-free area mass center coordinates derived from consecutive timeslots
   4.8. Detection of extreme shifts of cloud-free area mass centers
5. Case 29 July 2013
   5.1. Correlation between two IR consecutive images for 15, 5 and 2.5min scans

5.2. Correlation between two HRV consecutive images for 15, 5 and 2.5min scans
5.3. Mean IR values for full image, cloudy and clear atmosphere areas for 15, 5 and 2.5min scans
5.4. Mean HRV values for full image, cloudy and clear atmosphere areas for 15, 5 and 2.5min scans
5.5. Mean IR 2.5-5min scans differences for full image, cloudy and clear atmosphere areas
5.6. Mean HRV 2.5-5min scans differences for full image, cloudy and clear atmosphere areas
5.7. Time changes of cloud-free area mass center coordinates derived from consecutive timeslots
5.8. Detection of extreme shifts of cloud-free area mass centers

1. **Case 11-12 September 2012**

1.1. Correlation between two IR consecutive images for 15, 5 and 2.5min scans

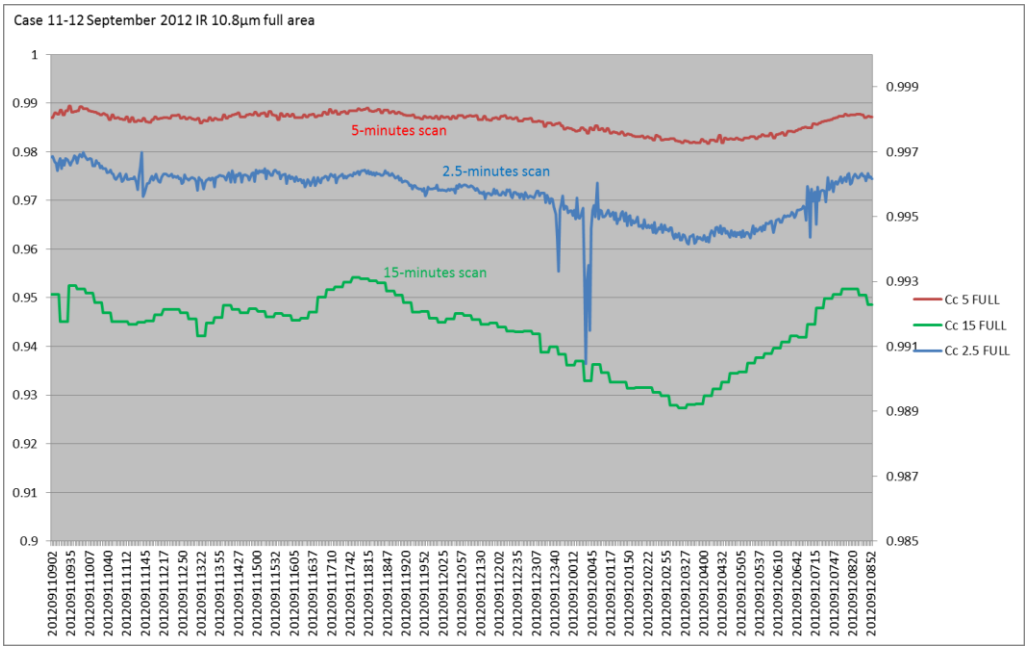

1.2. Correlation between two HRV consecutive images for 15, 5 and 2.5min scans

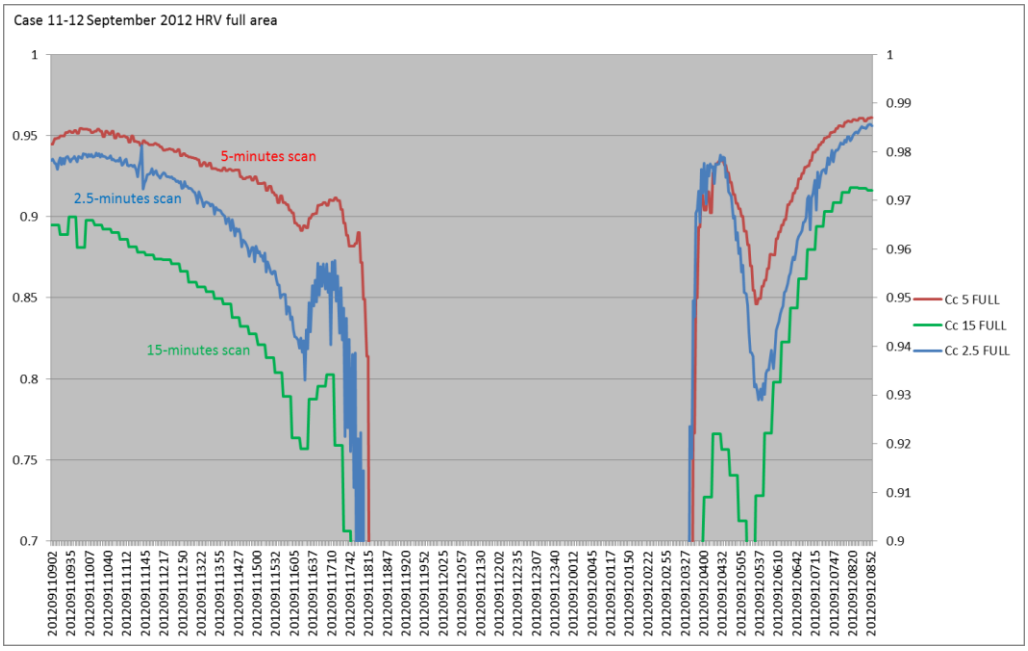

1.3. Mean IR values for full image, cloudy and clear atmosphere areas for 15, 5 and 2.5min scans

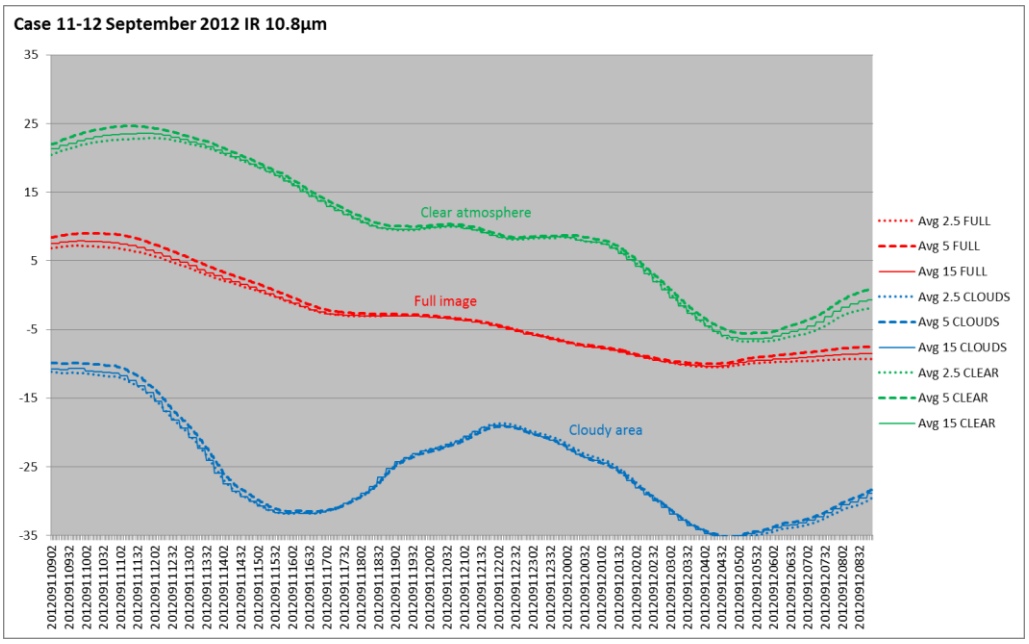

1.4. Mean HRV values for full image, cloudy and clear atmosphere areas for 15, 5 and 2.5min scans

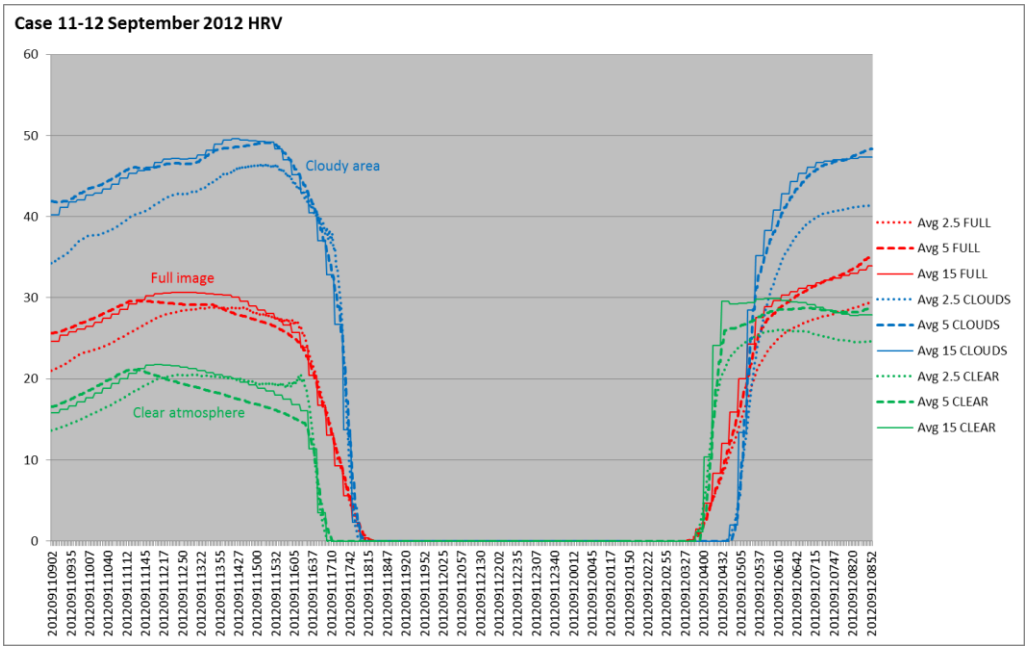

1.5. Mean IR 2.5-5min scans differences for full image, cloudy and clear atmosphere areas

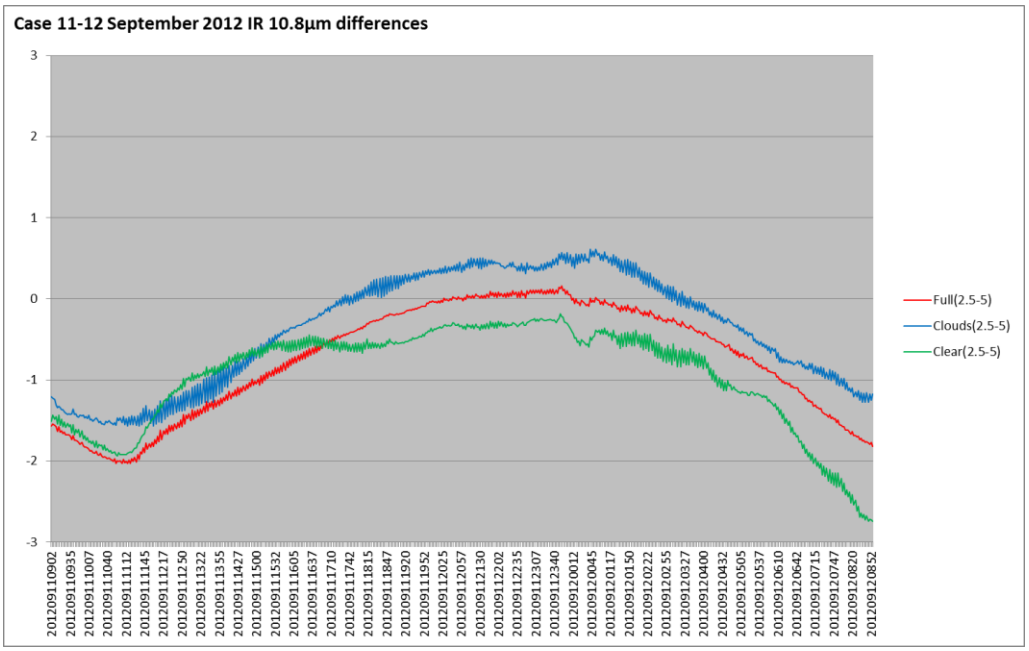

1.6. Mean HRV 2.5-5min scans differences for full image, cloudy and clear atmosphere areas

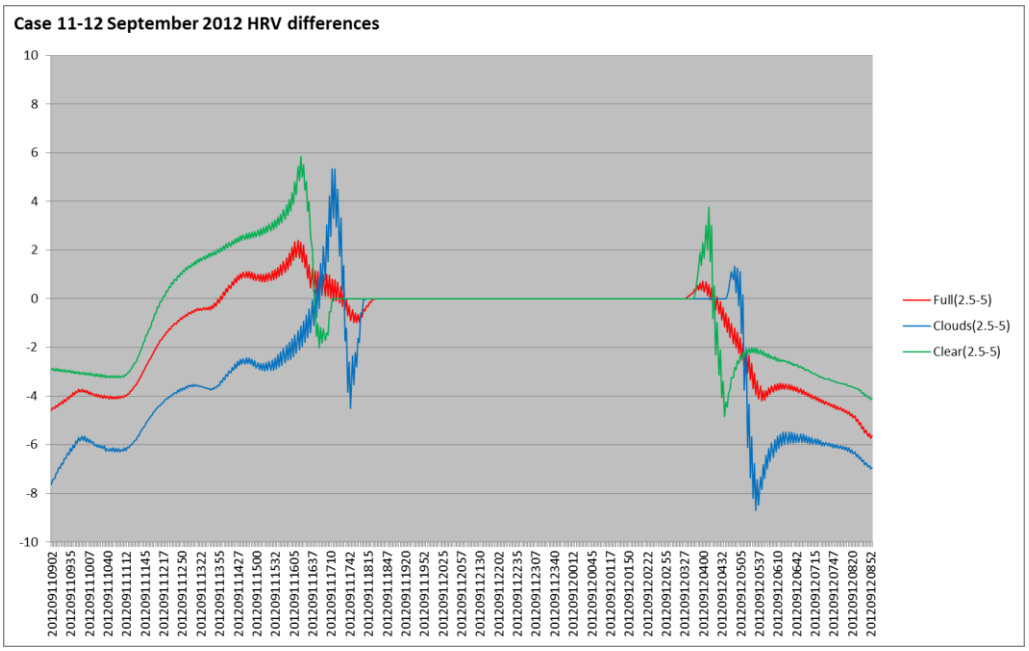

1.7. Time changes of cloud-free area mass center coordinates derived from consecutive timeslots

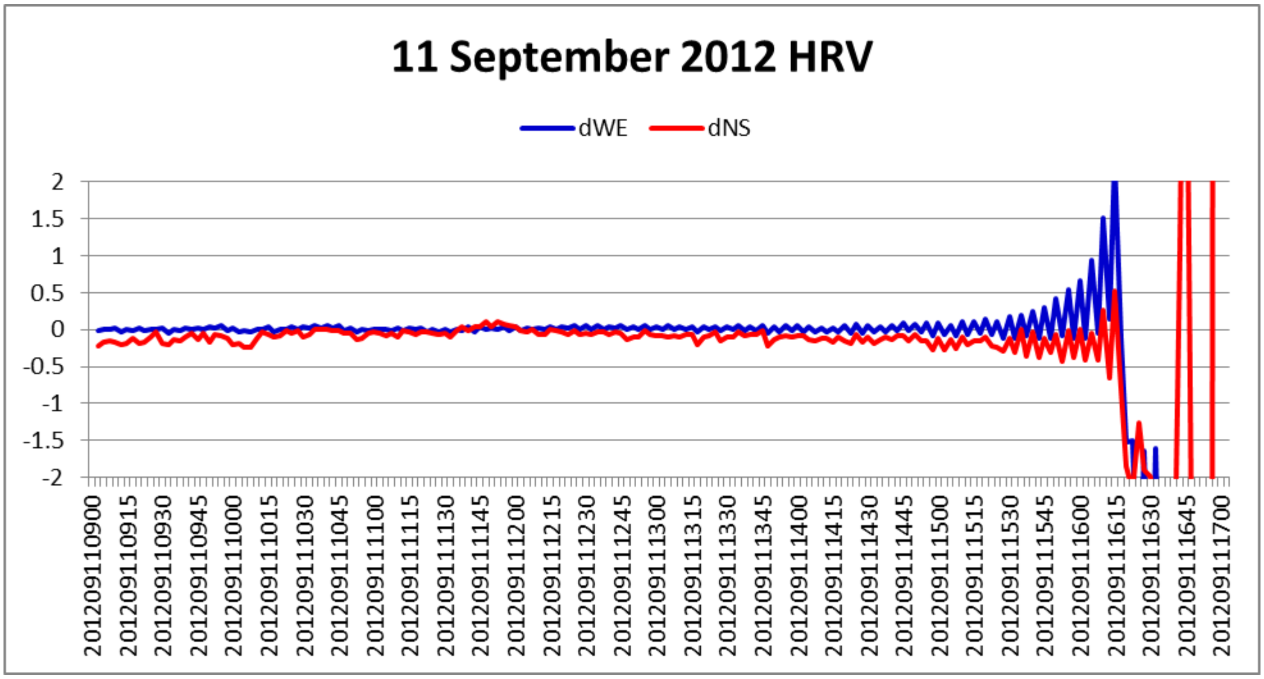

1.8. Detection of extreme shifts of cloud-free area mass centers

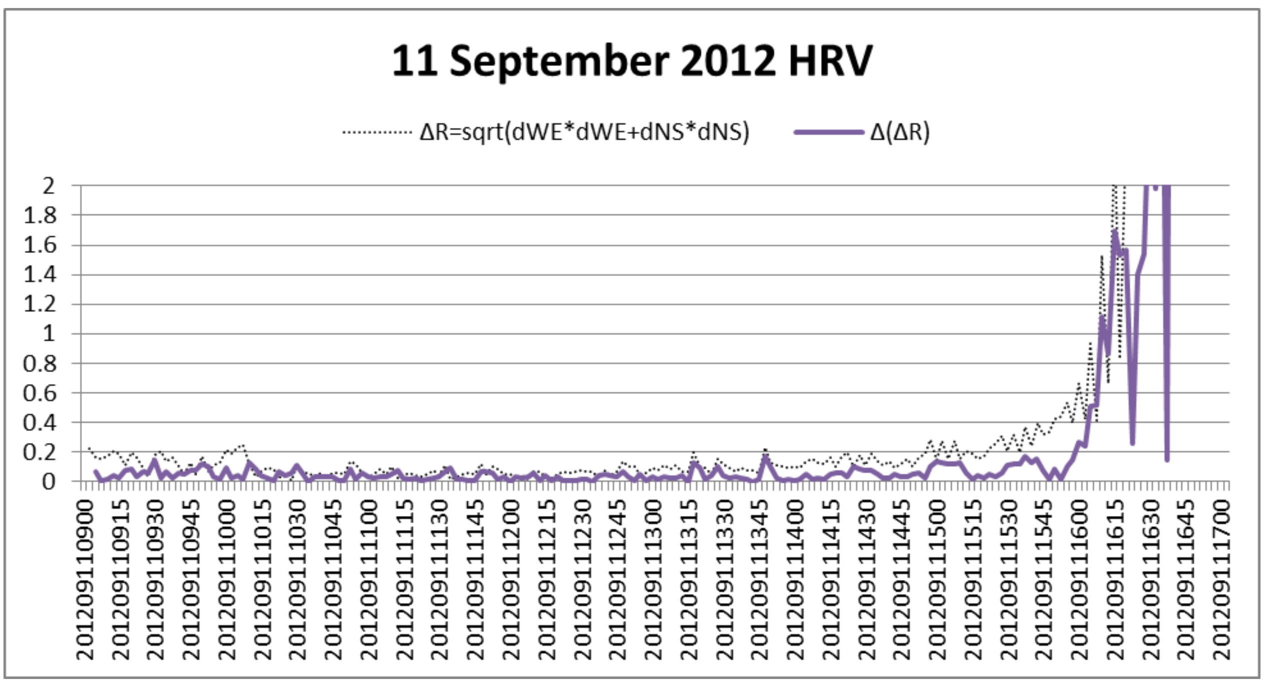

2. Case 17 May 2013

2.1. Correlation between two IR consecutive images for 15, 5 and 2.5min scans

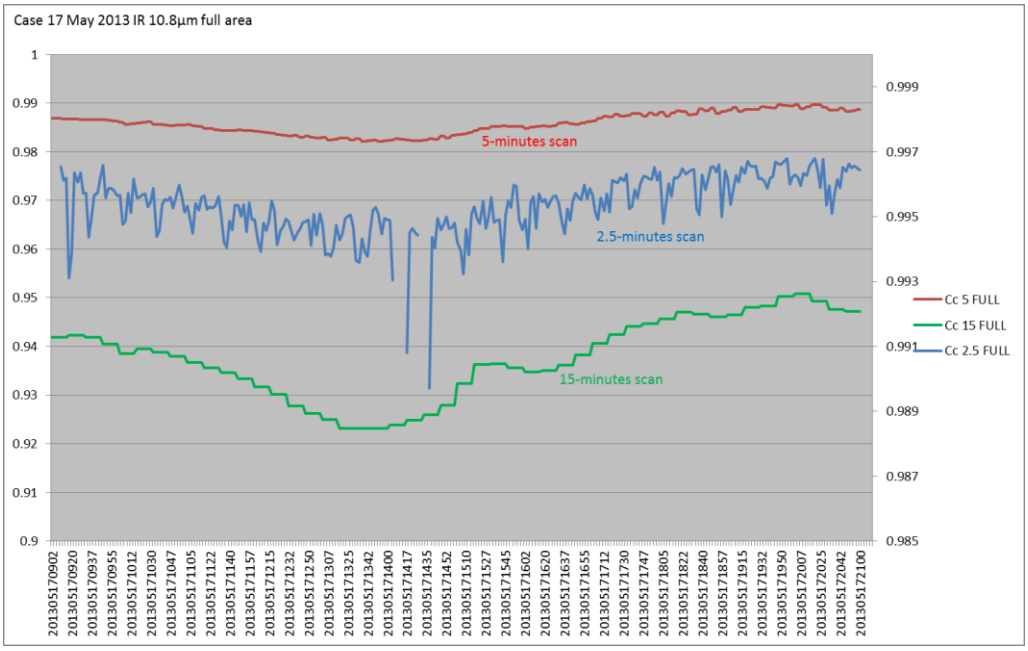

2.2. Correlation between two HRV consecutive images for 15, 5 and 2.5min scans

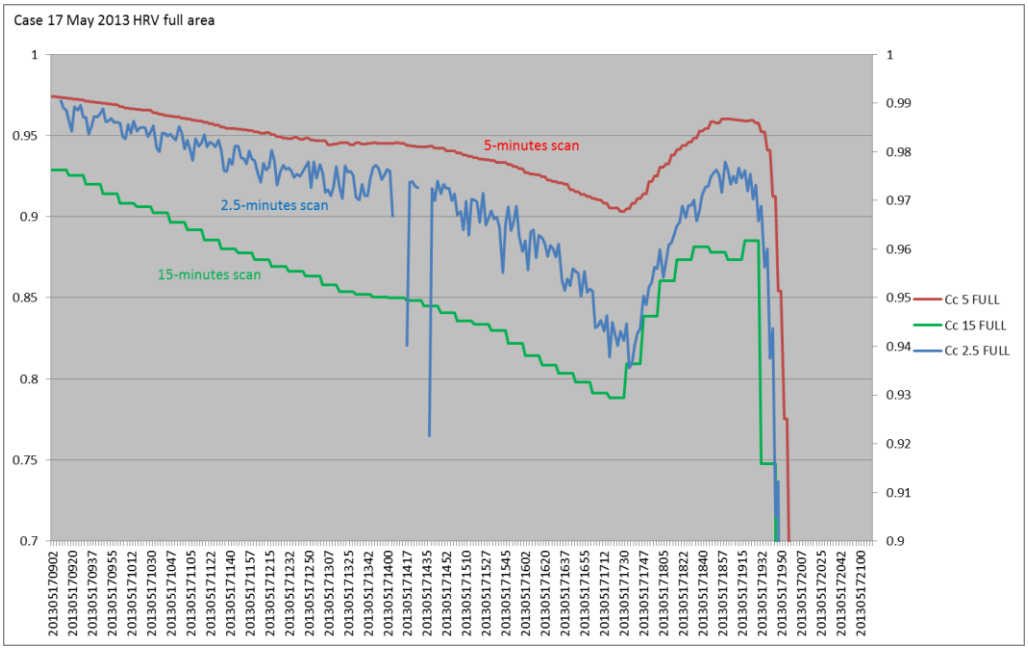

2.3. Mean IR values for full image, cloudy and clear atmosphere areas for 15, 5 and 2.5min scans

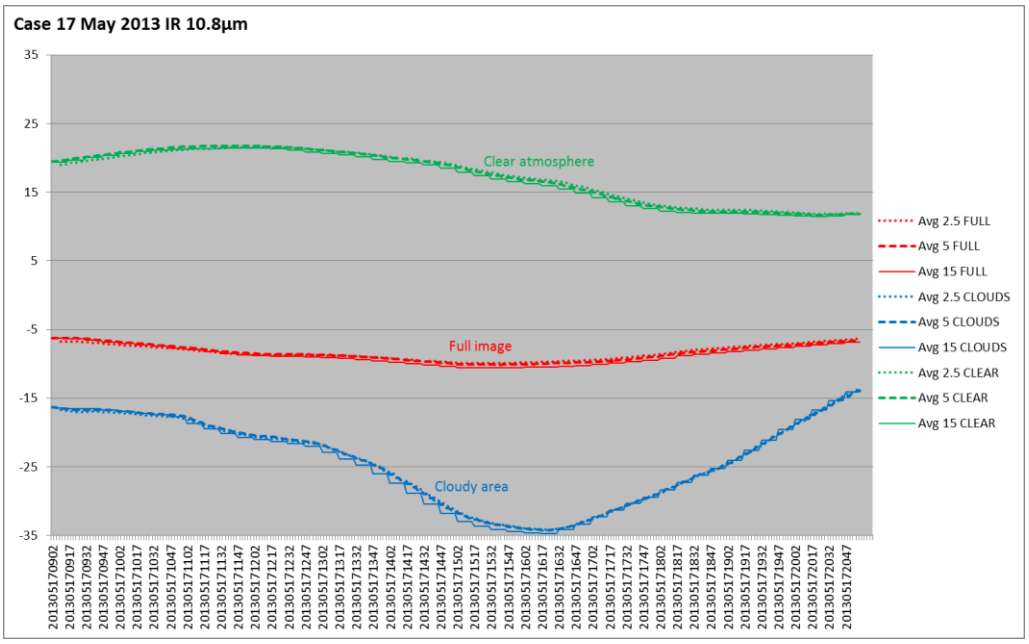

2.4. Mean HRV values for full image, cloudy and clear atmosphere areas for 15, 5 and 2.5min scans

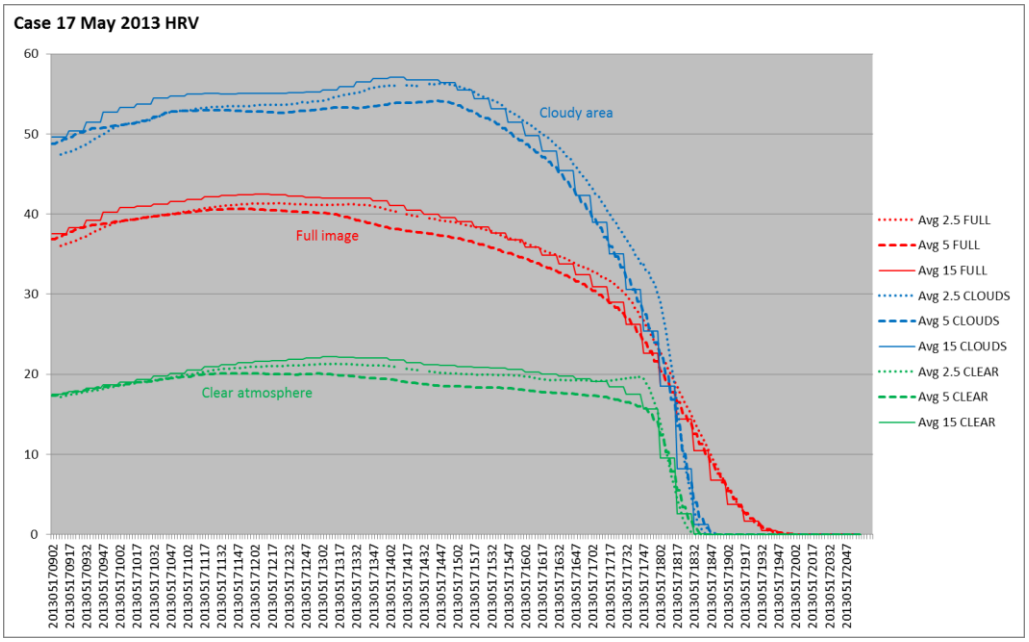

2.5. Mean IR 2.5-5min scans differences for full image, cloudy and clear atmosphere areas

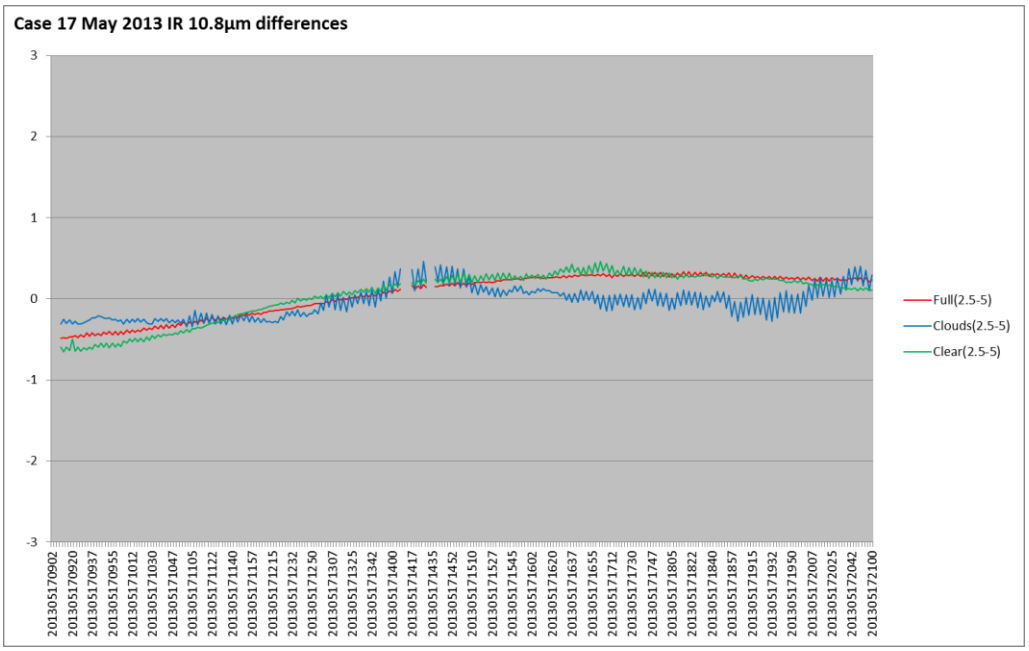

2.6. Mean HRV 2.5-5min scans differences for full image, cloudy and clear atmosphere areas

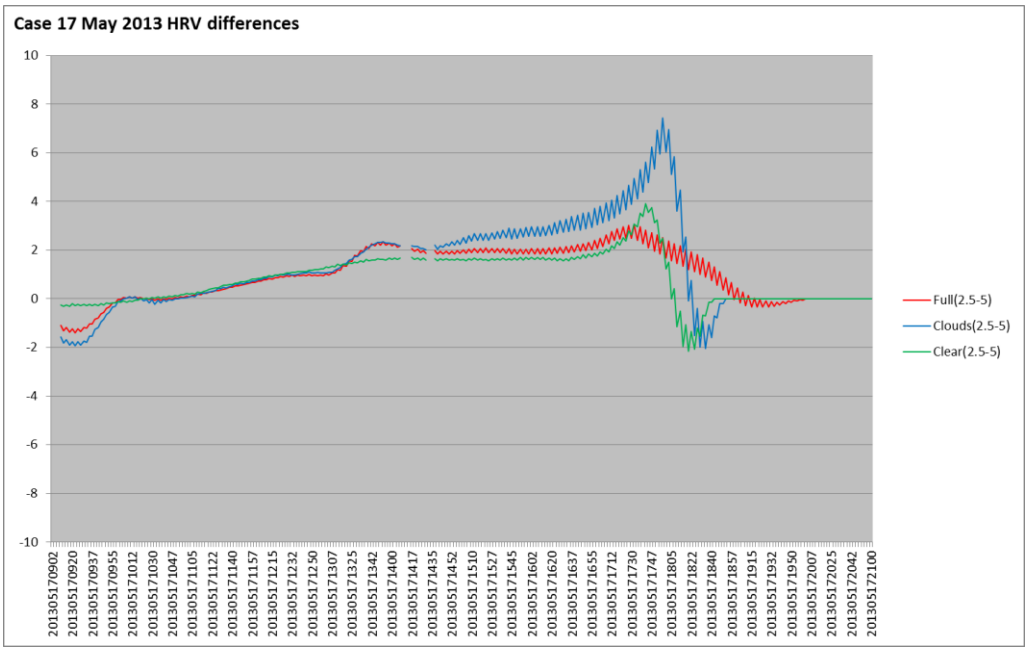

2.7. Time changes of cloud-free area mass center coordinates derived from consecutive timeslots

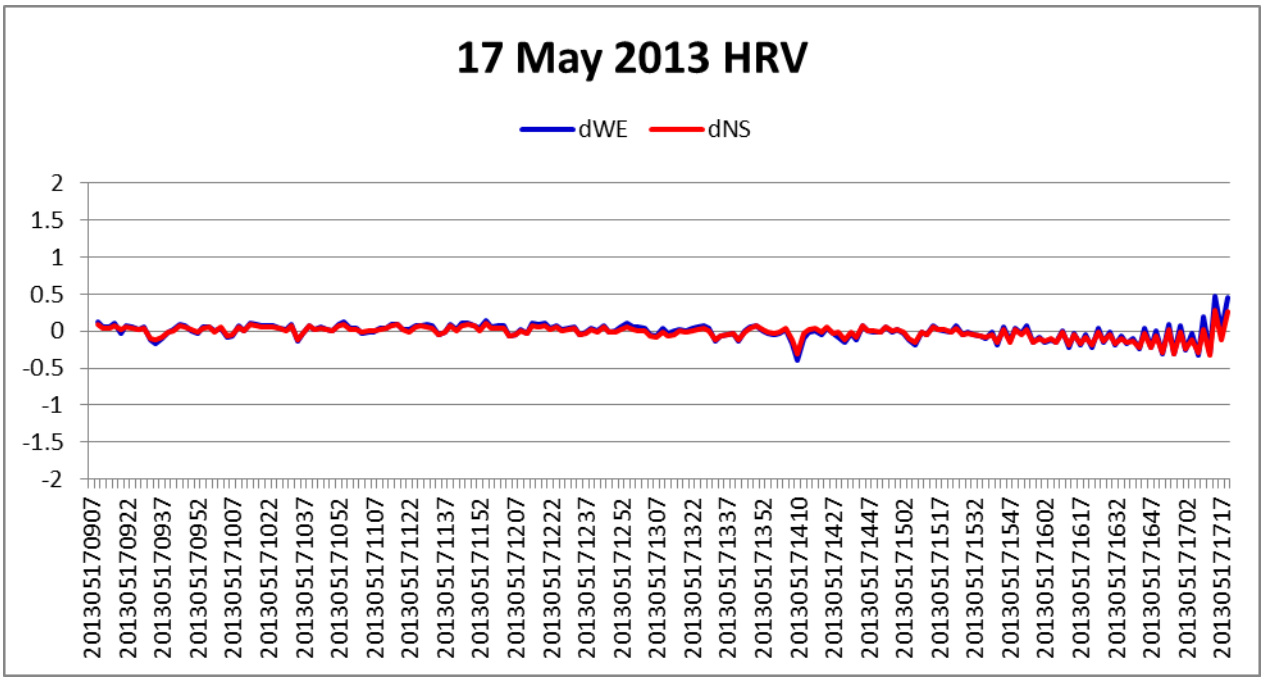

2.8. Detection of extreme shifts of cloud-free area mass centers

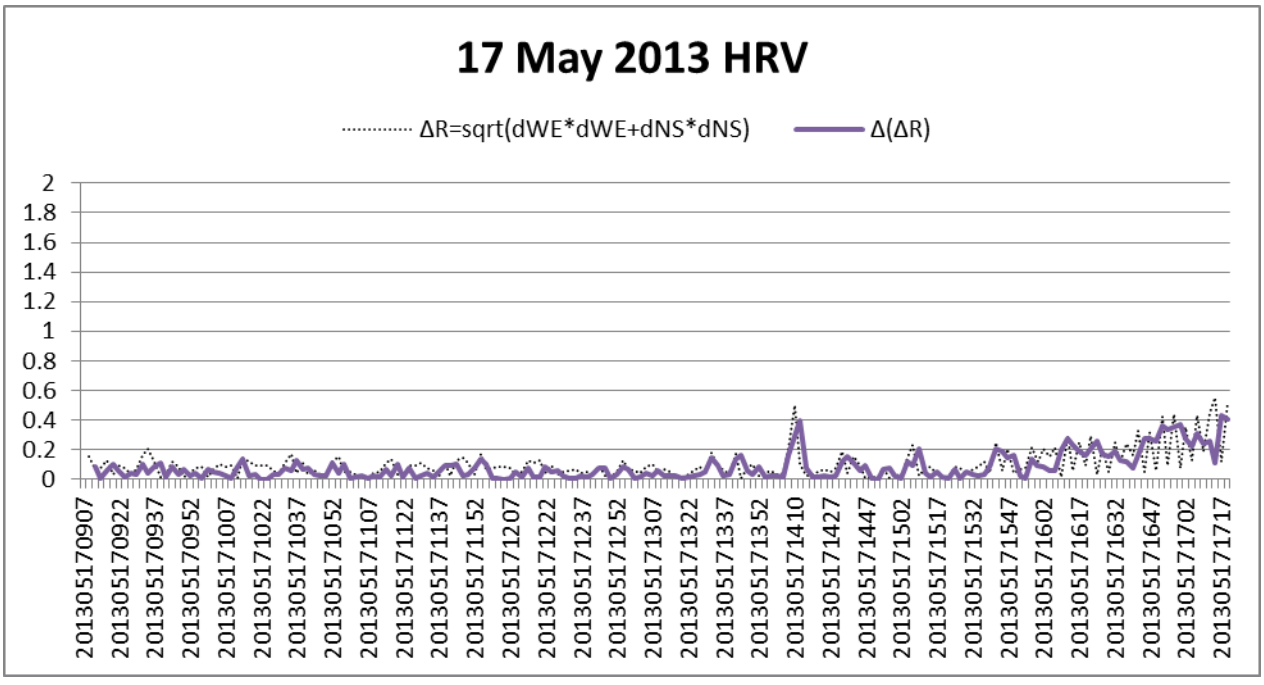

Case 17 June 2013

3.1. Correlation between two IR consecutive images for 15, 5 and 2.5min scans

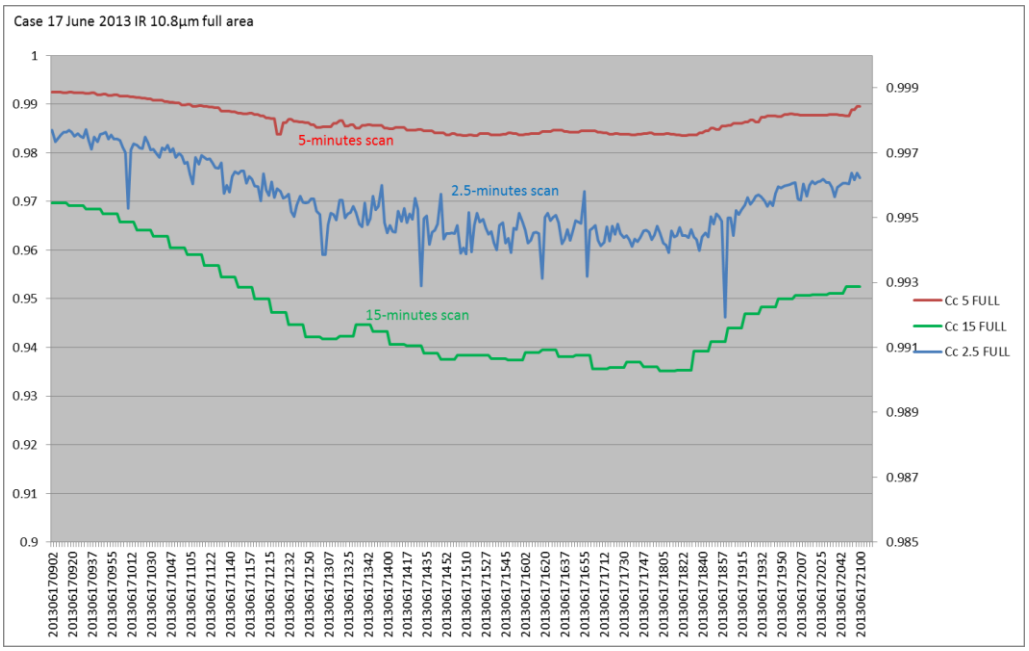

3.2. Correlation between two HRV consecutive images for 15, 5 and 2.5min scans

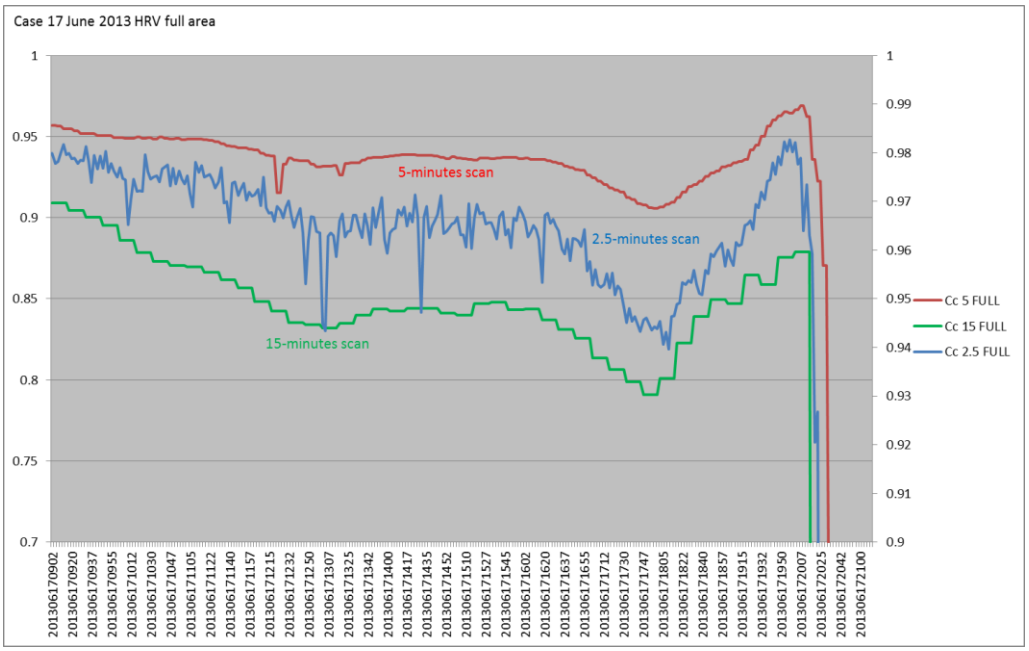

3.3. Mean IR values for full image, cloudy and clear atmosphere areas for 15, 5 and 2.5min scans

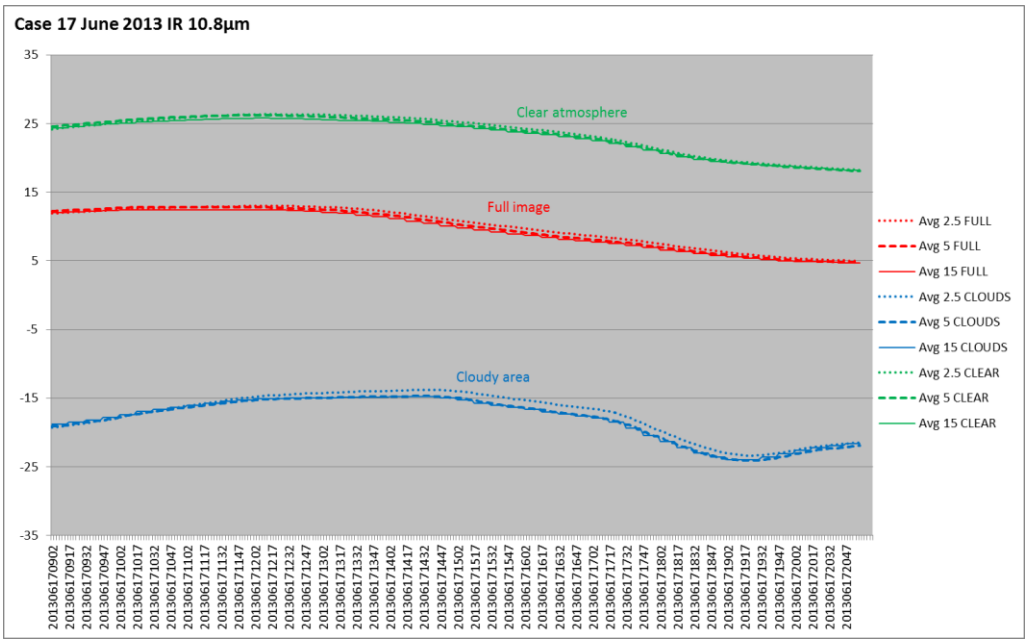

3.4. Mean HRV values for full image, cloudy and clear atmosphere areas for 15, 5 and 2.5min scans

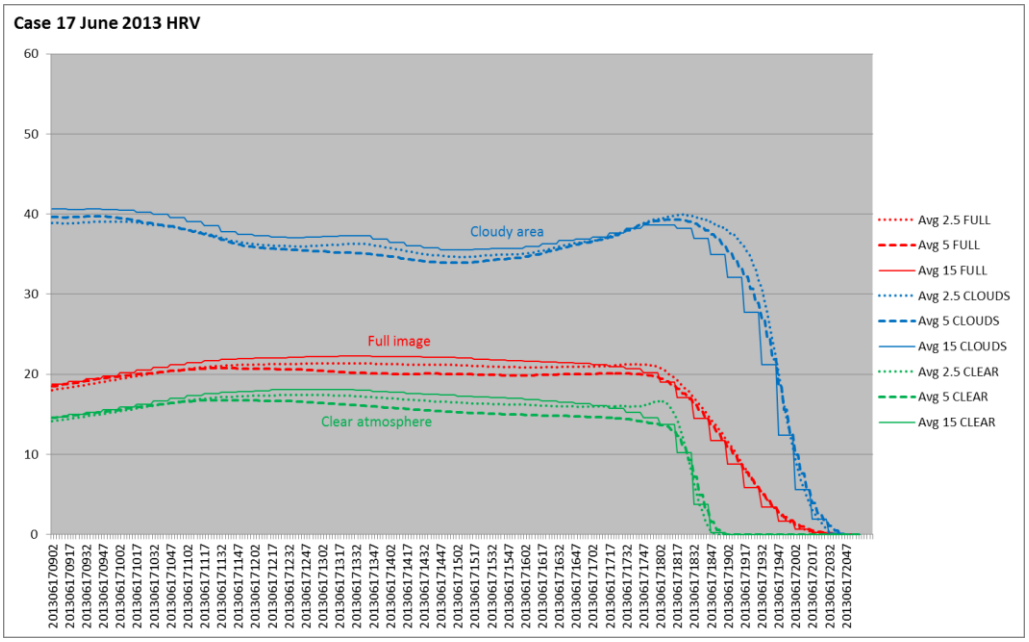

3.5. Mean IR 2.5-5min scans differences for full image, cloudy and clear atmosphere areas

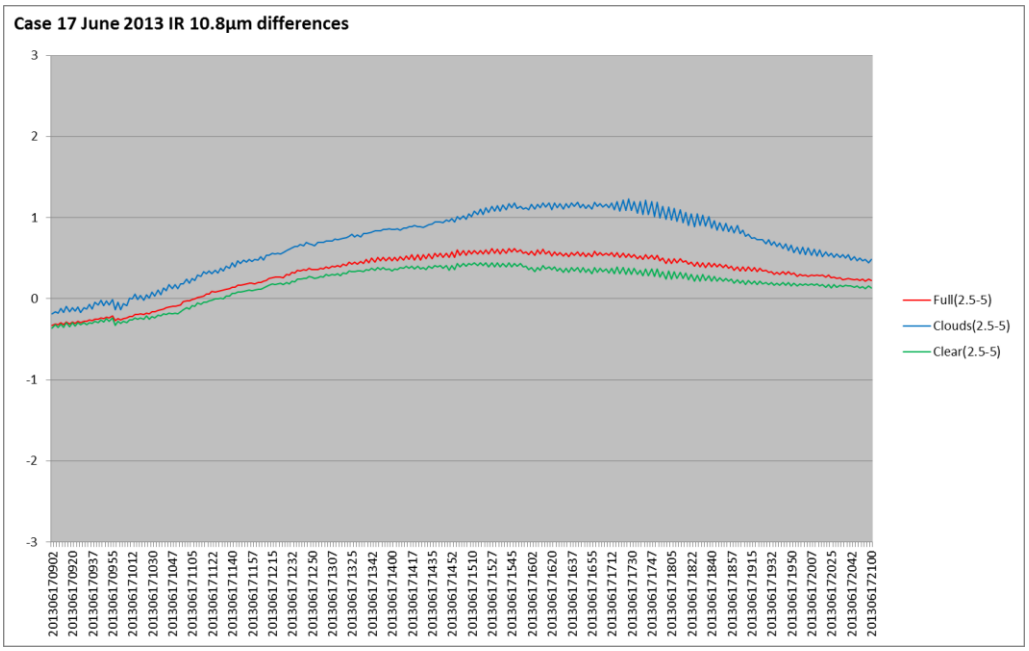

3.6. Mean HRV 2.5-5min scans differences for full image, cloudy and clear atmosphere areas

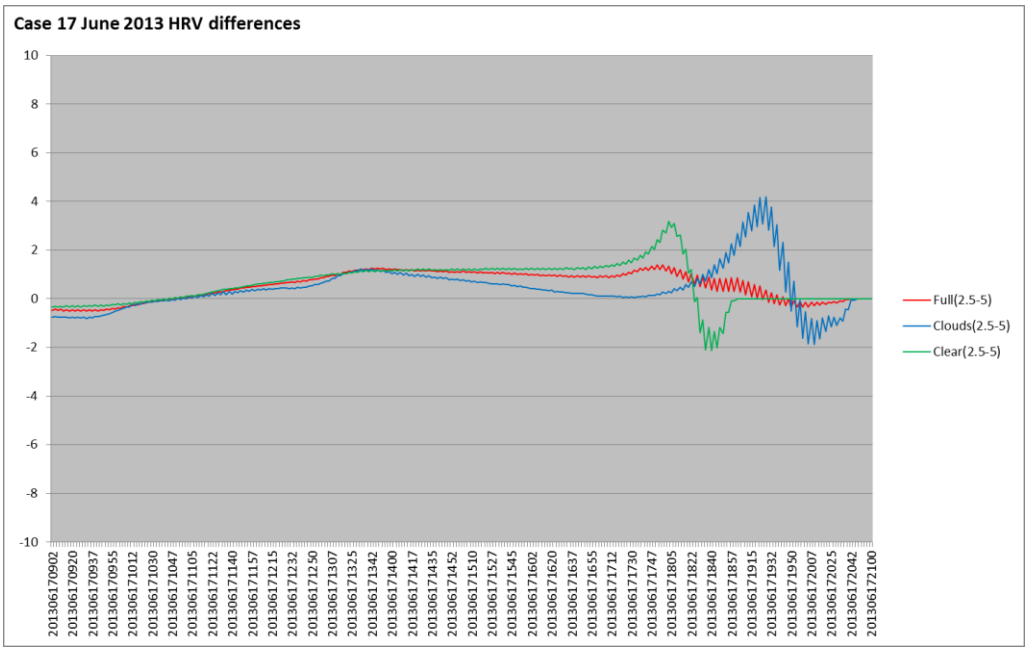

3.7. Time changes of cloud-free area mass center coordinates derived from consecutive timeslots

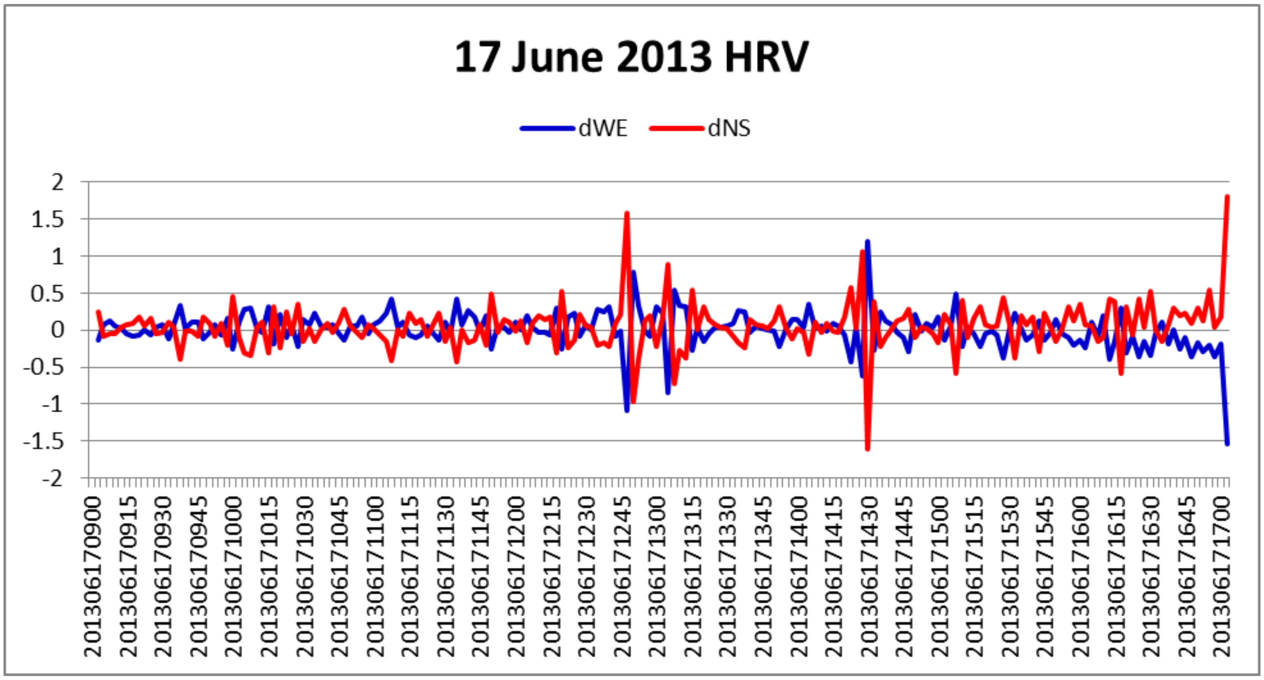

3.8. Detection of extreme shifts of cloud-free area mass centers

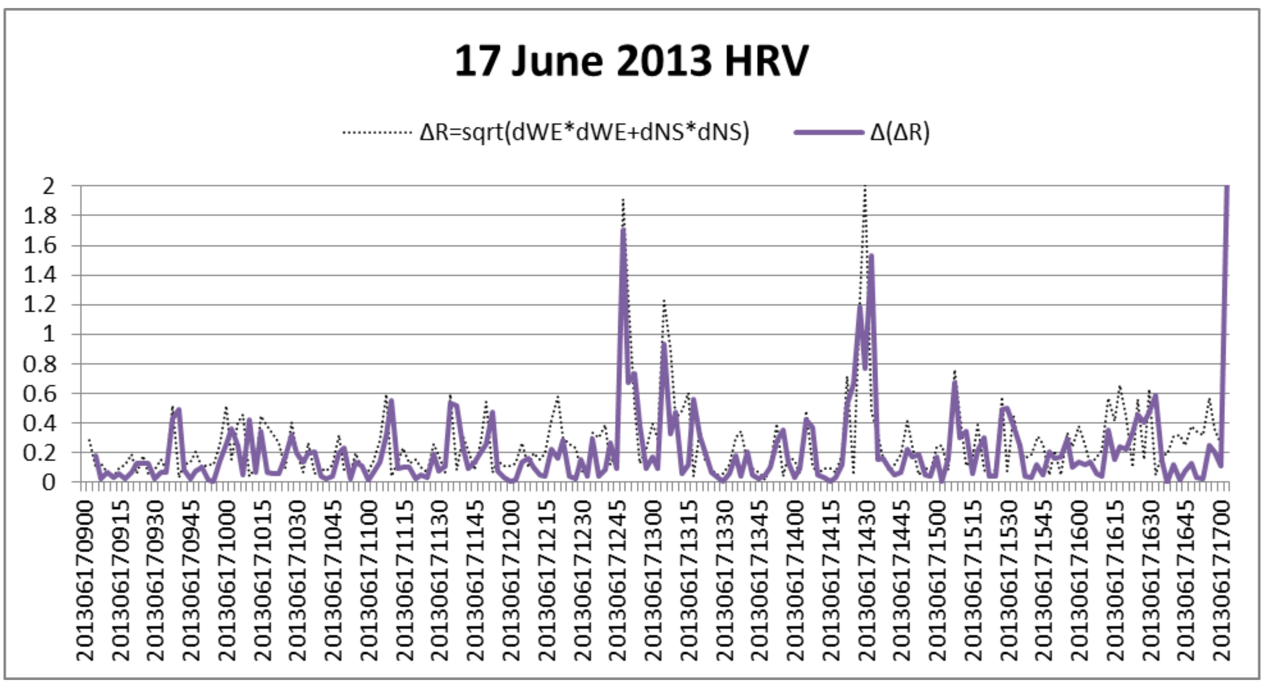

4. Case 20 June 2013

4.1. Correlation between two IR consecutive images for 15, 5 and 2.5min scans

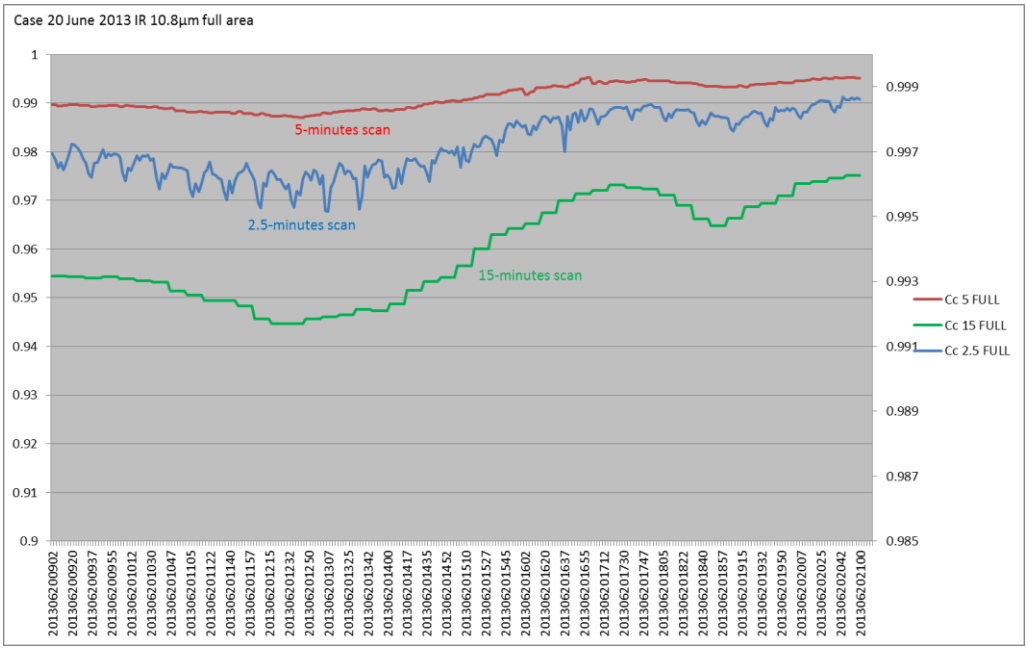

4.2. Correlation between two HRV consecutive images for 15, 5 and 2.5min scans

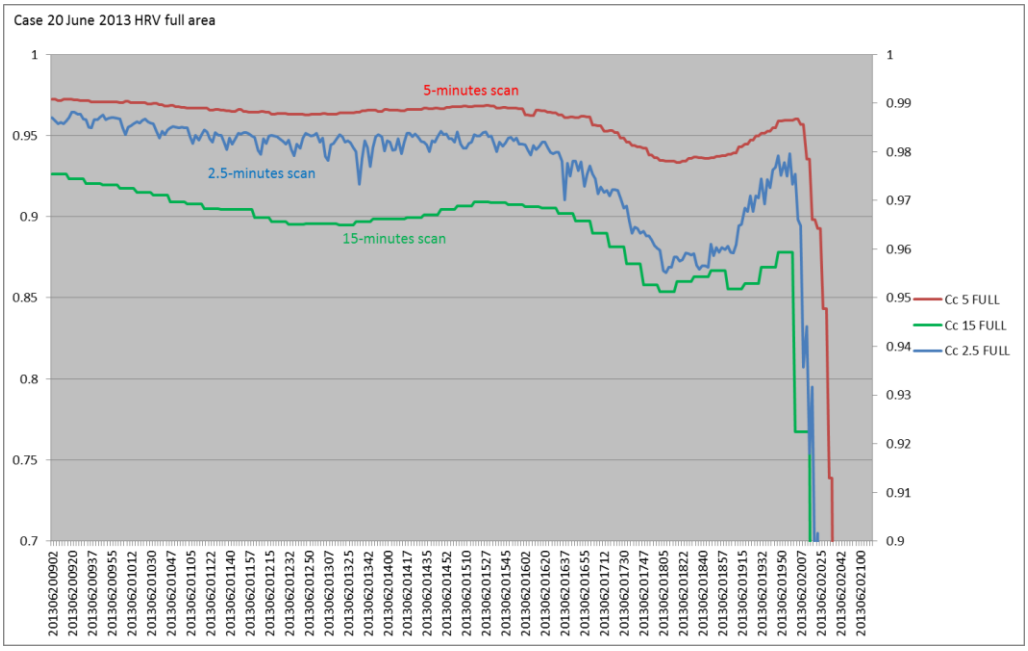

4.3. Mean IR values for full image, cloudy and clear atmosphere areas for 15, 5 and 2.5min scans

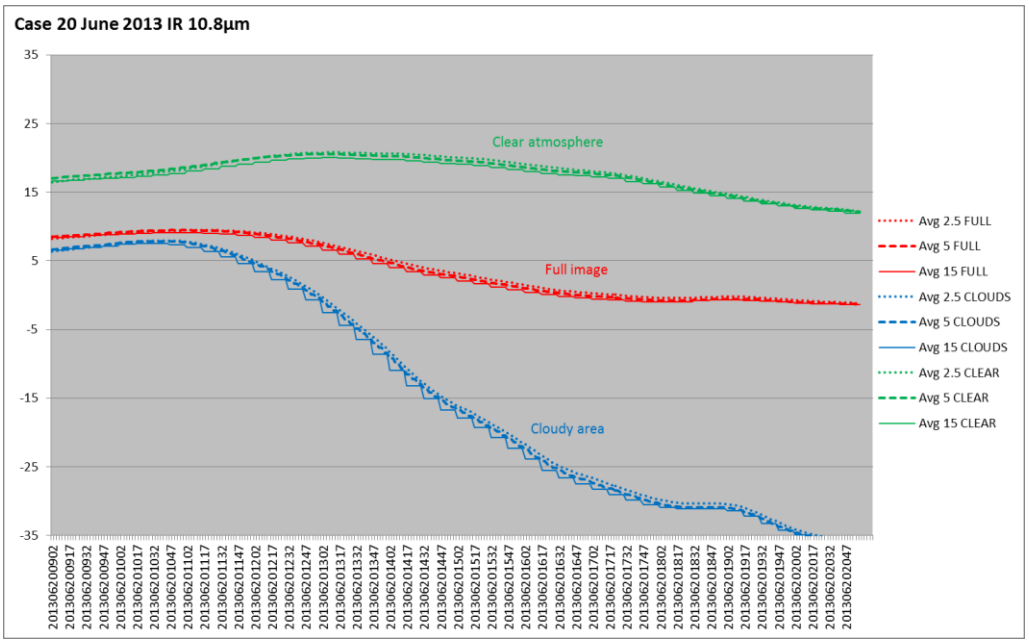

4.4. Mean HRV values for full image, cloudy and clear atmosphere areas for 15, 5 and 2.5min scans

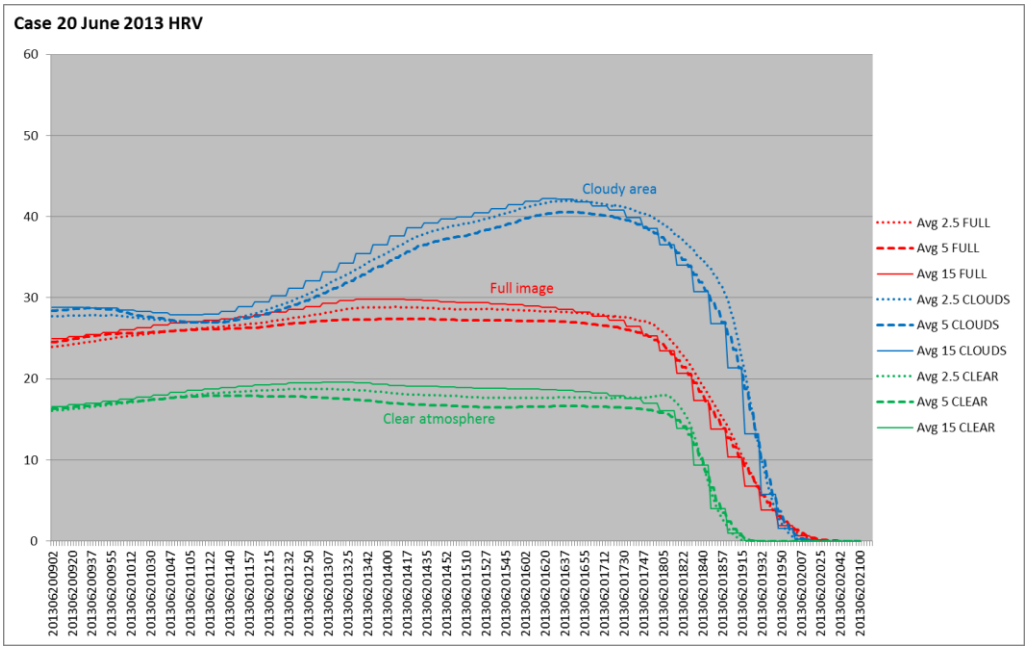

4.5. Mean IR 2.5-5min scans differences for full image, cloudy and clear atmosphere areas

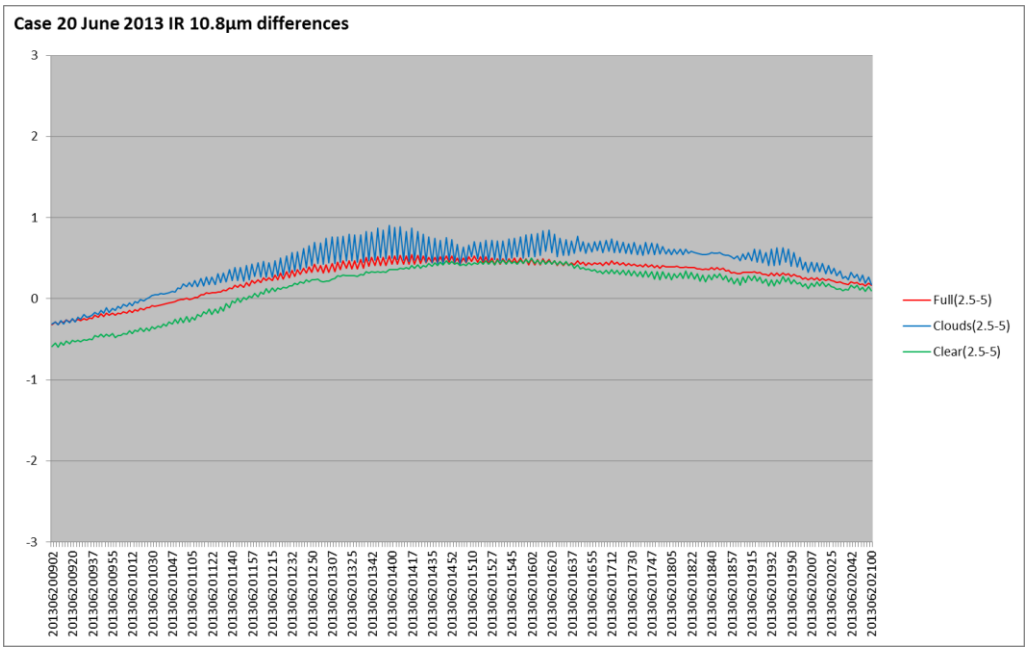

4.6. Mean HRV 2.5-5min scans differences for full image, cloudy and clear atmosphere areas

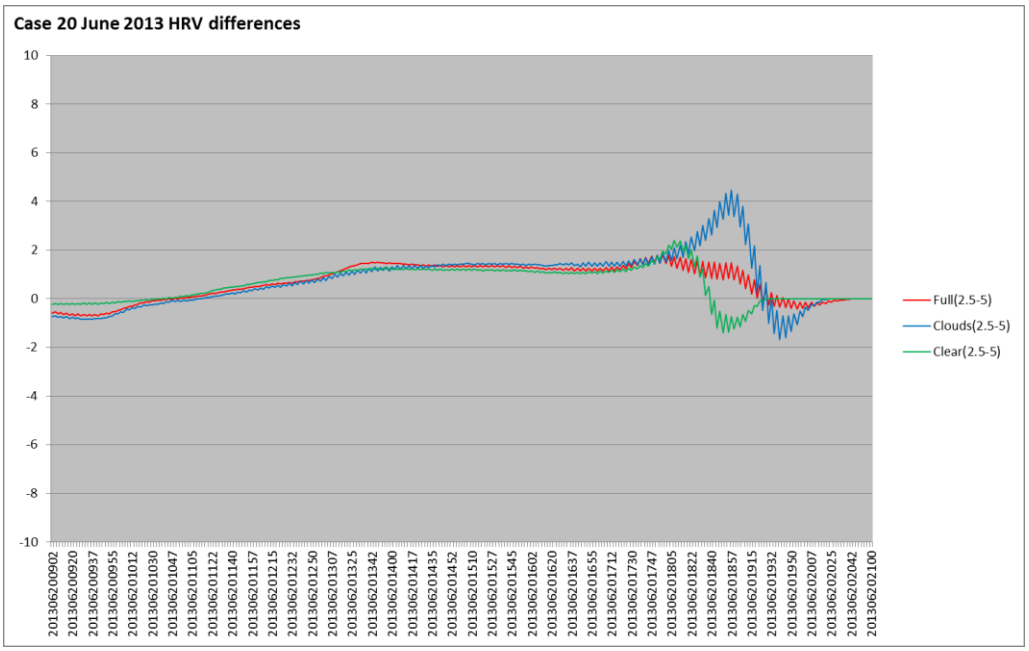

4.7. Time changes of cloud-free area mass center coordinates derived from consecutive timeslots

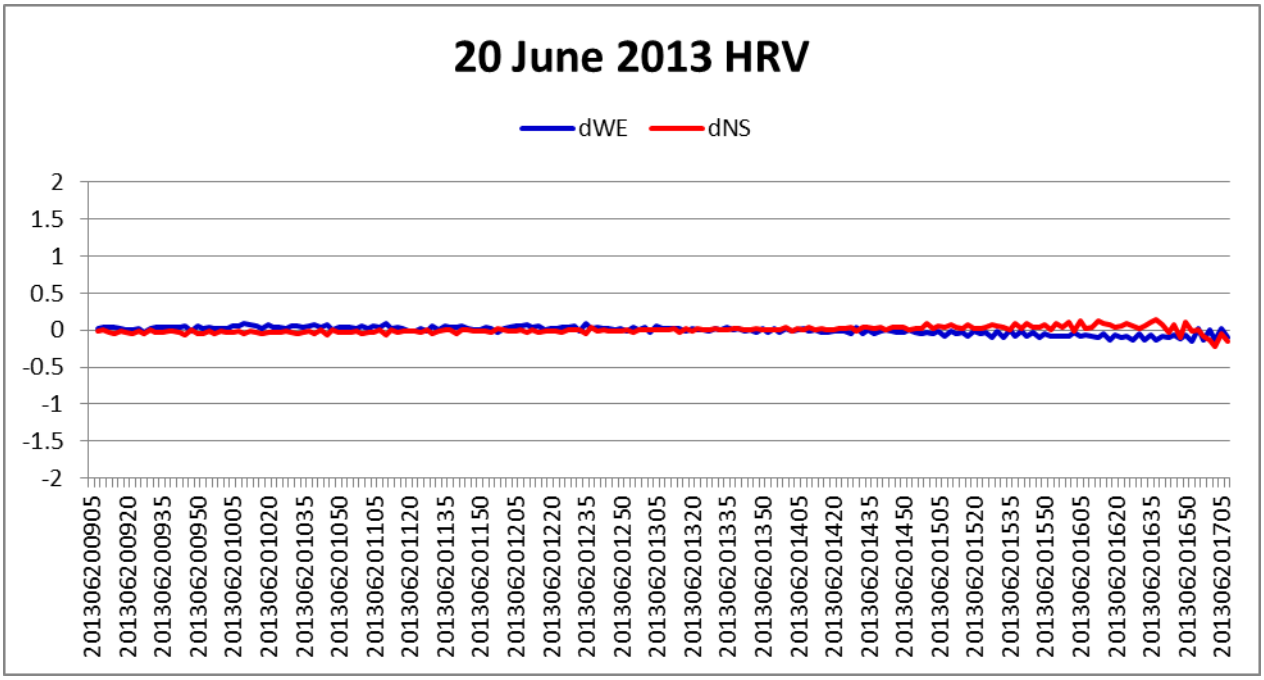

4.8. Detection of extreme shifts of cloud-free area mass centers

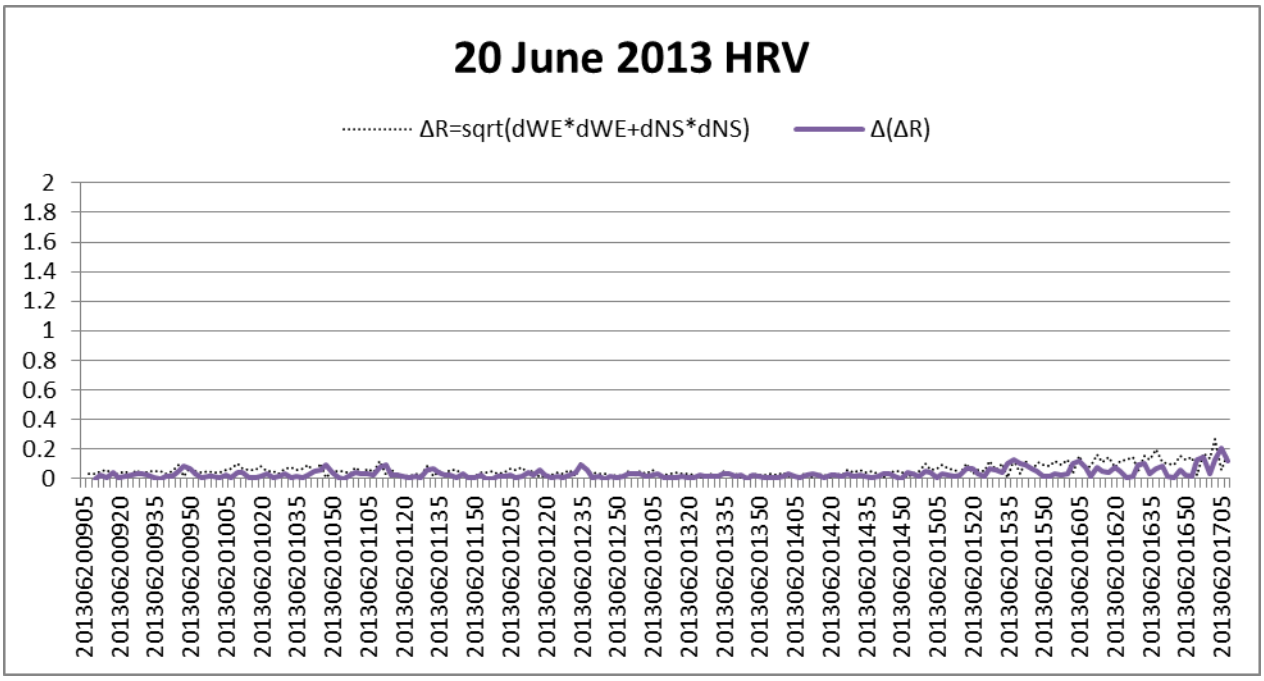

5. Case 29 July 2013

5.1. Correlation between two IR consecutive images for 15, 5 and 2.5min scans

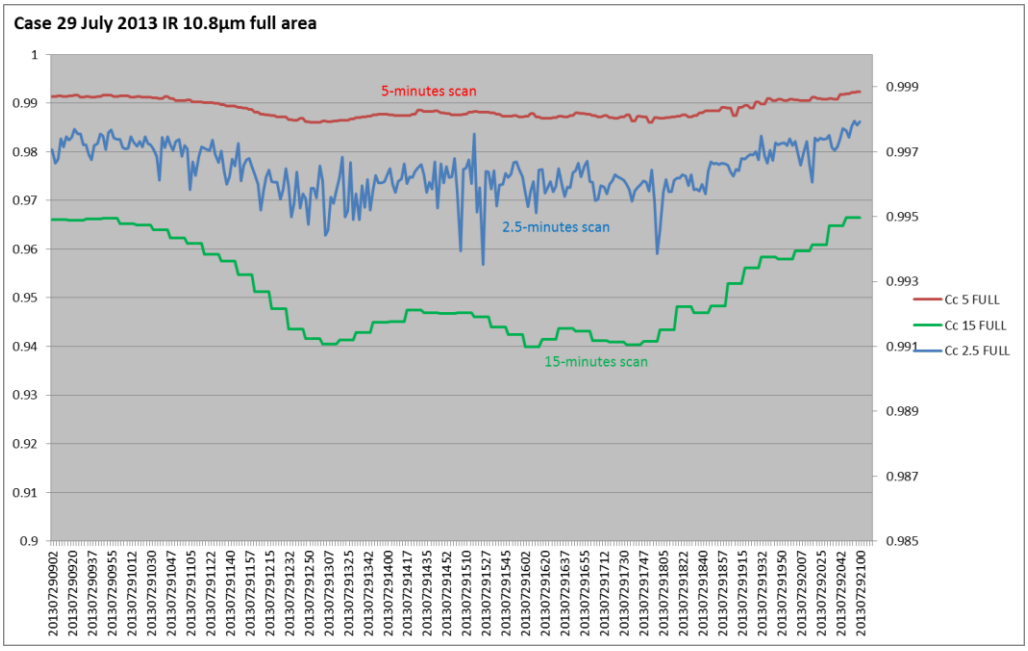

5.2. Correlation between two HRV consecutive images for 15, 5 and 2.5min scans

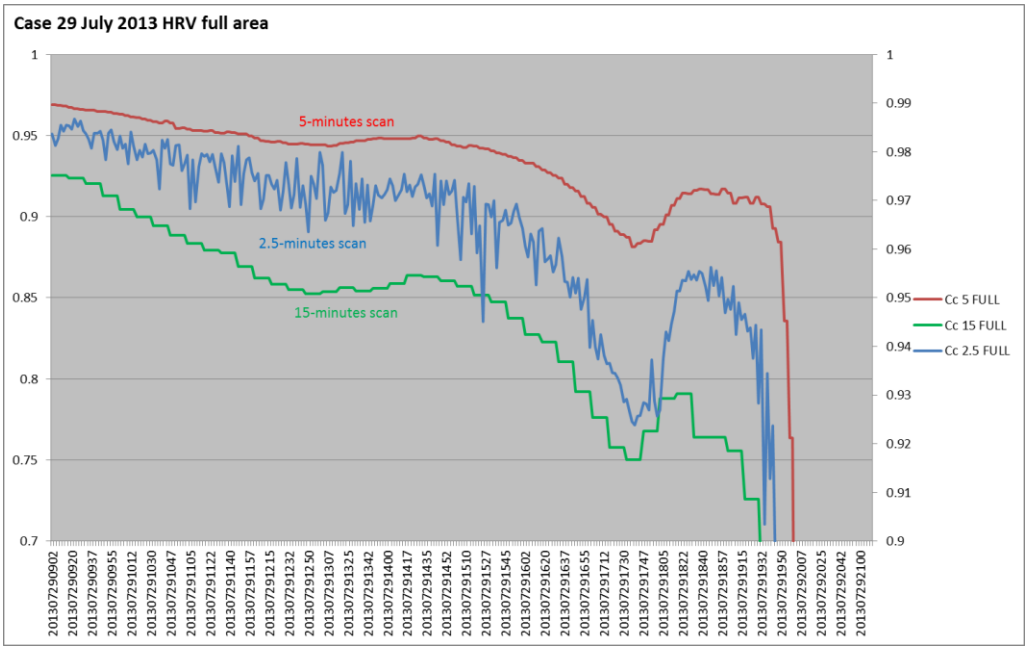

5.3. Mean IR values for full image, cloudy and clear atmosphere areas for 15, 5 and 2.5min scans

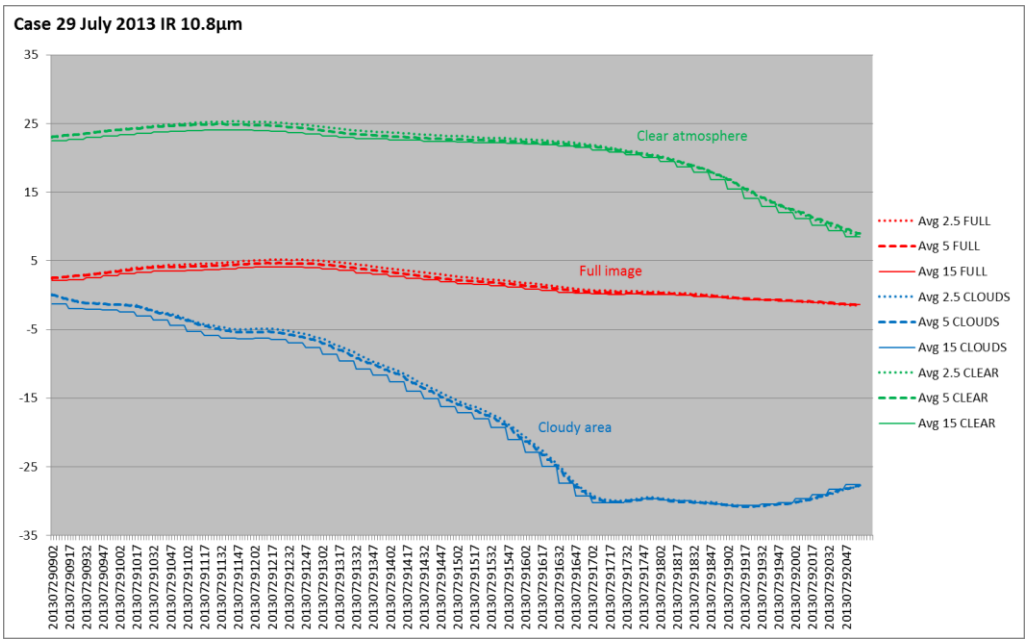

5.4. Mean HRV values for full image, cloudy and clear atmosphere areas for 15, 5 and 2.5min scans

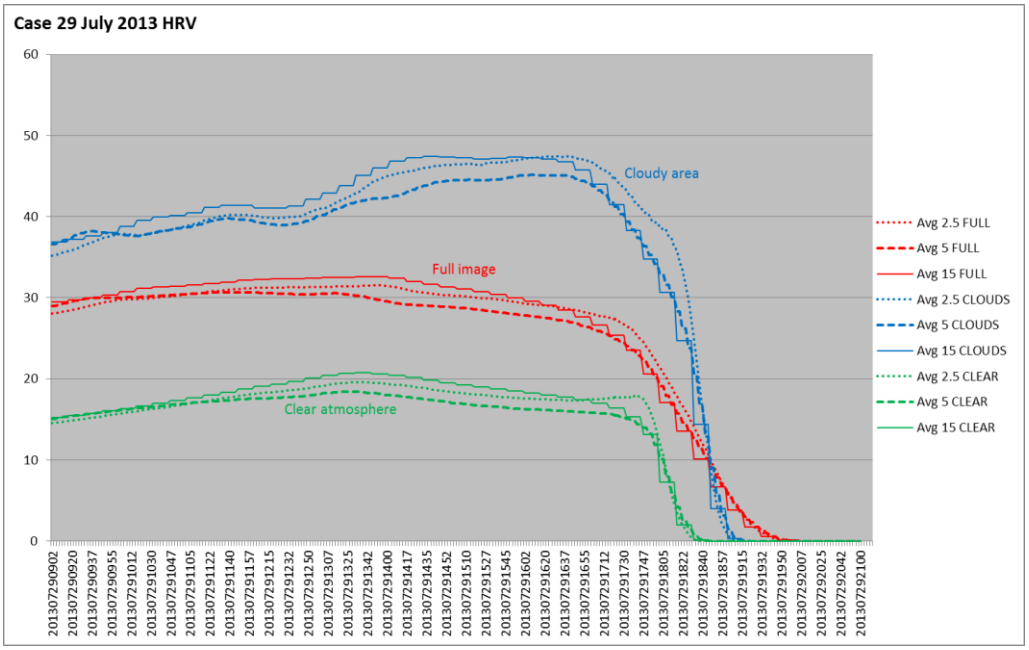

5.5. Mean IR 2.5-5min scans differences for full image, cloudy and clear atmosphere areas

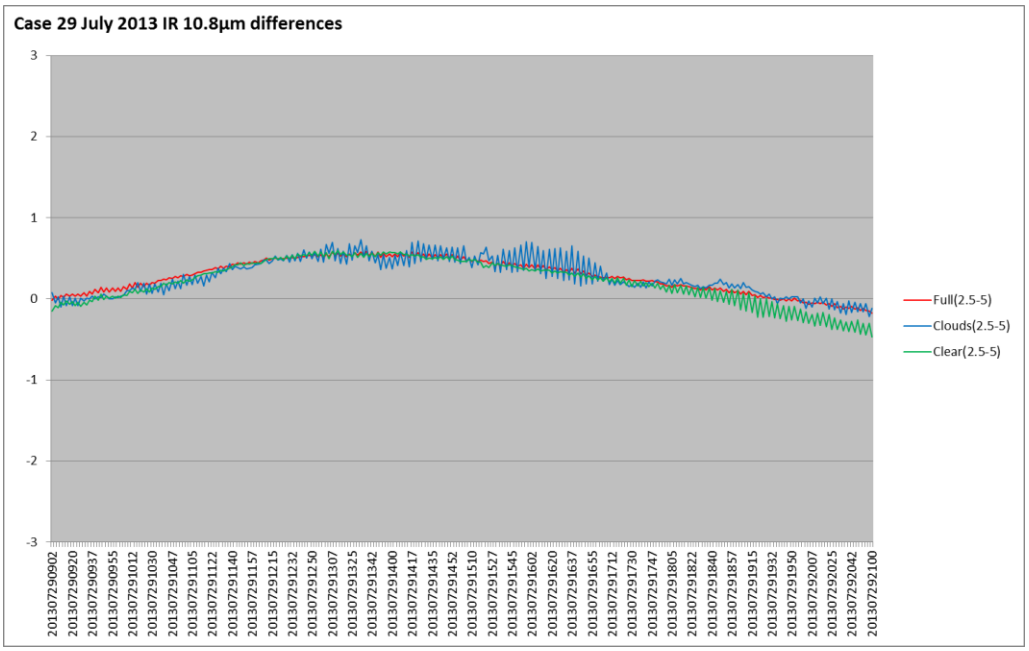

5.6. Mean HRV 2.5-5min scans differences for full image, cloudy and clear atmosphere areas

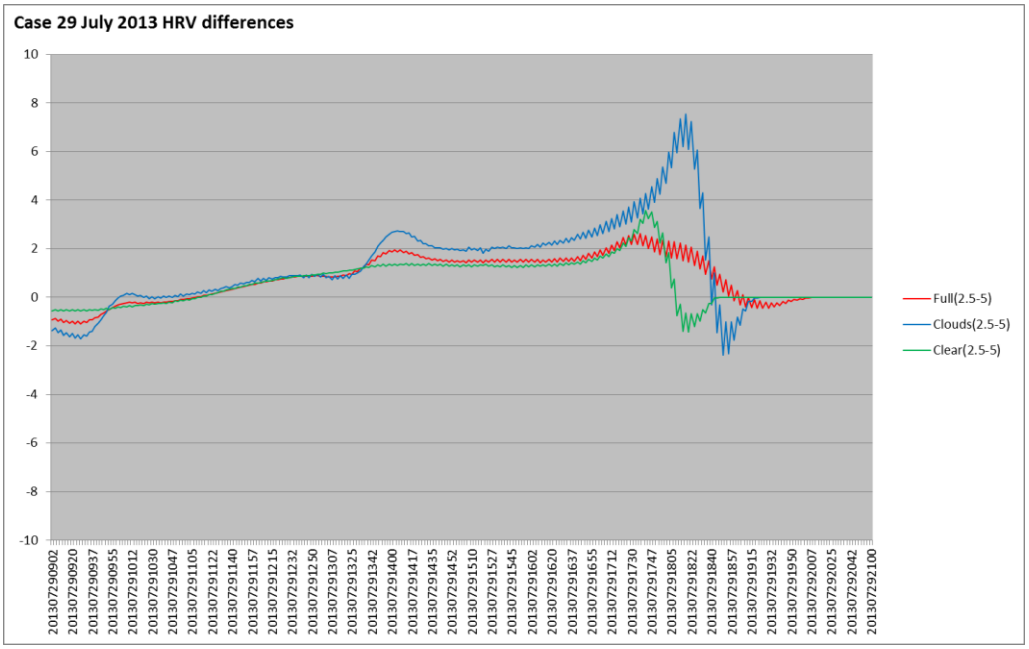

5.7. Time changes of cloud-free area mass center coordinates derived from consecutive timeslots

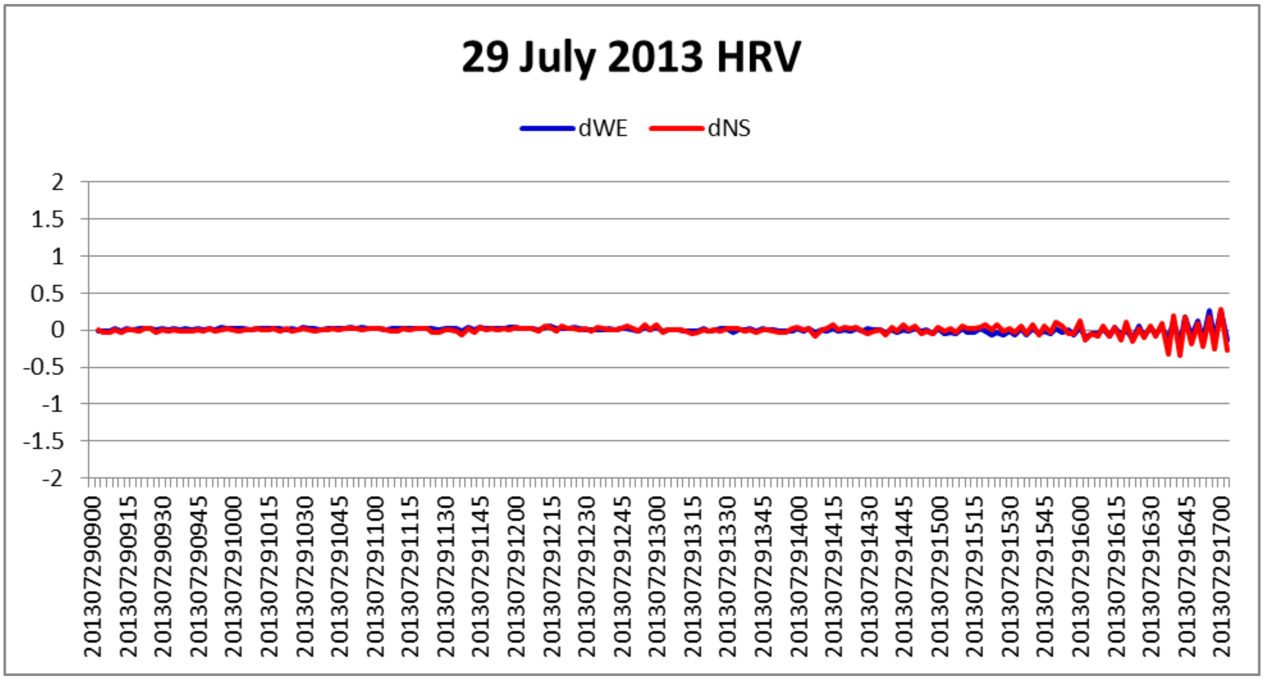

5.8. Detection of extreme shifts of cloud-free area mass centers